Frontiers in Science and Engineering

International Journal

Edited by The Hassan II Academy of Science and Technology of Morocco

Contents

ACADEMY Press MA

Volume 4 - Number 2 - 2014

Editorial board

Editor-in-Chief :
O. FASSI-FEHRI, Permanent Secretary, Hassan II Academy of Science and Technology, Morocco

Associate Editors-in-Chief :
M. BOUSMINA, Chancellor, Hassan II Academy of Science and Technology, Morocco
J. DERCOURT, Honorary Permanent Secretary, Académie des Sciences, France
C. GRISCELLI, Université René Descartes, France
D. OUAZAR, Ecole Mohammadia d'Ingénieurs, Université Mohammed V-Agdal, Rabat, Morocco (Executive director)

Associate Editors :

Mathematics, Applied Mathematics, Computer Sciences
D. ABOUTAJDINE, Faculté des Sciences, Université Mohammed V- Agdal, Rabat, Morocco
G. GAMBOLATTI, Universita Degli Studi di Padova, Italy
M. GHALLAB, Institut National de Recherche en Informatique et en Automatique (INRIA), France
Y. OUKNINE, Faculté des Sciences, Université Cadi Ayyad - Marrakesh, Morocco.
E. ZUAZUA, Basque Center for Applied Mathematics, Bilbao, Spain

Physics, Chemistry, Engineering Sciences
D. AIT KADI, Laval University, Canada
A. BENYOUSSEF, Faculté des Sciences, Université Mohammed V-Agdal, Rabat, Morocco
M. BOUSMINA, Chancellor, Hassan II Academy of Science and Technology, Morocco
E.M. ESSASSI, Faculté des Sciences, Université Mohammed V-Agdal, Rabat, Morocco
G.G. FULLER, Stanford University, California, USA
A. MAAZOUZ, Institut National de Sciences Appliquées, Lyon, France
D. OUAZAR, Ecole Mohammadia d'Ingénieurs, Université Mohammed V-Agdal, Rabat, Morocco
E.H. SAIDI, Faculté des Sciences, Université Mohammed V-Agdal, Rabat, Morocco
P.A. TANGUY, Ecole Polytechnique - Montréal (Canada) & Corporate Science & Technology, Total American Services Inc.Comité de - Houston (USA)

Life Sciences (Medical, Health, Agriculture, Biology, Genetics)
M. BESRI, Institut Agronomique et Vétérinaire Hassan II, Rabat, Morocco
T. CHKILI, Faculté de Médecine, Université Mohammed V-Souissi, Rabat, Morocco
R. EL AOUAD, Faculté de Médecine, Université Mohammed V-Souissi, Rabat, Morocco
C. GRISCELLI, Institut Necker, Faculté de Médecine, Université René Descartes, France
A. SASSON, GID, Paris, France
A. SEFIANI, Institut National d’Hygiène, Rabat, Morocco

Earth, Water and Oceans, Environmental Sciences
M. AIT KADI, Conseil Général du Développement Agricole, Rabat, Morocco
A. CHENG, University of Mississipi, USA
F. EL BAZ, Boston University, USA
A. EL HASSANI, Institut Scientifique, Rabat, Morocco
R.T. HANSON, USGS, USA
T. OUARDA, Masdar Institute of Technology, Masdar City, Abu Dhabi, United Arab Emirates
M.S. VASCONCELOS, EU Fisheries, Portugal

Strategic Studies and Economic Development
N. EL AOUFI, Faculté des Sciences Juridiques, Economiques et Sociales, Université Mohammed V-Agdal, Rabat, Morocco
M. BERRIANE, Faculté des Lettres et des Sciences Humaines, Université Mohammed V-Agdal, Rabat, Morocco
K. SEKKAT, Université Libre de Bruxelles, Belgique

Frontiers in Science and Engineering
International Journal

Edited by The Hassan II Academy of Science and Technology of Morocco

Contents

Dépôt légal : 2012 PE 0007
ISSN : 2028 - 7615

ACADEMY Press MA

Email : fse@academiesciences.ma
www.academiesciences.ma/fse/

Layout by : AGRI-BYS S.A.R.L (A.U)
Printed by : Imprimerie LAWNE
11, rue Dakar, 10040 - Rabat

WELCOME TO FSE

Frontiers in Science and Engineering, an International Journal edited by The Hassan II Academy of Science and Technology uses author-supplied PDFs for all online and print publication.

The objective of this electronic journal is to provide a platform of exchange of high quality research papers in science and engineering. Though it is rather of wide and broad spectrum, it is organized in a transparent and simple interactive manner so that readers can focus on their direct interest.

All papers are submitted to the normal peer-review process. Publication criteria are based on :
i) Novelty of the problem or methodology and problem solving, **ii**) Salience of the approach and solution technique, **iii**) Technical correctness and outputs, **iv**) Clarity and organization.

Papers are first reviewed by the Executive Board Director who receives the paper and, if relevant in terms of the overall requirements, it is then proposed to one of the most appropriate associate editor on the field who will select 2 to 3 expert reviewers. Electronic printing will allow considerable time savings for submission delays which will be reduced drastically to less than three to six months. Prospective authors are therefore invited to submit their contribution for assessment while subjected to similar quality criteria review used in paper journals.

Authors are notified of acceptance, need for revision or rejection of the paper. It may be noted that papers once rejected cannot be resubmitted. All the details concerning the submission process are described in another section. This electronic journal is intended to provide :

- the announcement of significant new results,
- the state of the art or review articles for the development of science and technology,
- the publication of proceedings of the Academy or scientific events sponsored by the Academy,
- the publication of special thematic issues.

So that the scientific community can :

- promptly report their work to the scientific community,
- contribute to knowledge sharing and dissemination of new results.

The journal covers the established disciplines, interdisciplinary and emerging ones. Articles should be a contribution to fundamental and applied aspects, or original notes indicating a significant discovery or a significant result.

The topics of this multidisciplinary journal covers amongst others :
Materials Science, Mathematics, Physics, Chemistry, Computer sciences, Energy, Earth Science, Biology, Biotechnology, Life Sciences, Medical Science, Agriculture, Geosciences, Environment, Water, Engineering and Complex Systems, Science education, Strategic and economic studies, and all related modeling, simulation and optimization issues, etc. ...

Once, a certain number of papers in a specific thematic, is reached, the Academy might edit a special paper issue in parallel to the electronic version.

PRESENTATION NOTE

Frontiers in Science and Engineering is an International Journal published by Hassan II Academy of science and Technology. In its nature, it is a multidisciplinary scientific journal and follows the rule of Frascatti international science classification of scientific areas.

Our Online Publications System Manager is an electronic publications system of an open access journal providing trimester/semester/annual publications of papers in all areas of the major aspects.

However as this covers a wide spectrum, we will restrict ourselves to 5 major areas:

- **Mathematics, Computer Science and Computational Applications (GRIS)+**
- **Physics, Chemistry and Engineering Sciences**
- **Life Sciences (Medical, Health, Agriculture, Biology, Genetics)**
- **Earth Sciences (Earth, Water and Oceans, Environmental Sciences)**
- **Strategic Studies and Economic Development**

All papers are subjected to peer-review by members of an editorial board or qualified reviewers and if accepted will be published in less than two months time.

The multi-journal welcomes the submission of manuscripts that meet the general scope and criteria's as described in our website.

The authors will be noticed the decision of manuscripts within 4 weeks after submission. Accepted articles will normally be published during the next 4 weeks.

Publication Fee: free

For more and detailed information please visit : http://www.academie.hassan2.sciences.ma/fse/

INTRODUCTION

In this issue of Frontiers in Science and Engineering International Journal, four papers are edited, two of them are dealing with mathematics and applications while the other two are for organic chemistry and materials.

The first paper entitled “Derivation of new chemotaxis models by asymptotic” presents a new approach to derive macro-scale models in biology using appropriate developments of kinetic theory and statistical mechanics at the cellular scale.

In the second paper entitled “The structure of some 2-groups and the capitulation problem for certain biquadratic fields”, the capitulation problem for certain number fields K of degree 4 is studied and followed by the determination of the structures of some 2-groups as an application.

The third paper entitled “Synthesis and UV-Visible complexation study of 1-pyrazolylbenzimidazol-2-one polyether macrocyclic derivatives” deals with a new polyether macrocyclic of 1-pyrazolylbenzimidazol-2-ones 5-6 that have been synthesized by the reaction of dichloro(poly)ethylene glycol in phase transfer catalysis conditions. The structure of these compounds were also identified.

In the fouth paper entitled “Atomic relaxation studying in Ag and Cu systems with (100) and (110) orientation”, the atomic relaxation in copper and silver Substrates are thoroughly investigated.

The Editiors

Derivation of new chemotaxis models by asymptotic analysis of kinetic models for large binary cell mixtures

N. Bellomo [1] **and A. Bellouquid**[2]

[1] Department of Mathematics, Faculty of Science, King Abdulaziz University, Jeddah, Saudi Arabia
[2] Cadi Ayyad University, Ensa, Marrakech, Morocco
[3] *Corresponding Author E-mail: a.bellouquid@uca.ma*

Abstract. *This paper deals with the derivation of macroscopic tissue models from the underlying description delivered by a class of equations modeling, by methods of the kinetic theory, binary mixtures of multi-cellular systems. The analysis refers to a suitable parabolic approximation to show how the macroscopic tissue behavior can be described from the underlying cellular description. The approach is specifically focused on the modeling of classical chemotaxis phenomena, and the chemotaxis–fluid.*

Key words: kinetic theory, multicellular systems, micro-macro asymptotic, Keller and Segel models.

1. Introduction

The derivation of biological macro-scale tissue models has been arguably introduced by the pioneering paper by Othmer, Dunbar and Alt [35]. Subsequently, several papers have contributed to further development of this research line, which consists in deriving microscopic models for multi cellular systems derived by methods of the generalized kinetic theory. Among others [3, 4, 7, 10, 12, 14, 22, 25, 32, 36], and several others as reported in the survey [6].

The derivation is based on suitable development of asymptotic methods, somehow analogous to those of the classical kinetic theory, which amount to expanding the distribution function in terms of a small dimensionless parameter related to the intermolecular distances (the space-scale dimensionless parameter), which is equivalent to the connections between the biological constants. The limit is singular and the convergence properties can be proved under suitable technical assumptions.

This present paper develops a different approach based on the kinetic-fluid formulation of equations. This micro-macro decomposition problem is well known in kinetic theory. The method is proposed for a binary mixture of cell populations to obtain a mixed parabolic–parabolic macroscopic model. However, the approach can be easily generalized to more than two populations.

More in details, the strategy consists in rewriting the kinetic equation as a coupled system of kinetic part and macroscopic one, by using the micro-macro decomposition of the distribution function. Indeed, this function is decomposed into its corresponding equilibrium distribution plus the deviation. By using a classical projection technique (as in the Chapmann–Enskog expansion), we obtain an evolution equation for the macroscopic parameters of the equilibrium coupled to a kinetic equation for the non-equilibrium part. This idea has been used to design a numerical scheme that preserves both the compressible Euler and Navier-Stokes asymptotic for the Boltzmann equation of rarefied gas dynamics in [33].

Our approach is rather general to apply to a very large class of equations modeling binary mixtures of multi-cellular systems, moreover it gives the exact order of approximation of the kinetic model by the corresponding macroscopic one. In particular, it consists in deriving the diffusion processes for both population: the classical Keller–Segel model [27, 28, 29, 30], the drift optimal Keller–Segel model [5], and a chemotaxis model with saturated chemotaxis flux [17], and pressureless hyperbolic description (direct drift coupling).

The aim of this paper, is to prove that our approach can be extended to a broader class of equations modeling binary mixtures of multi-cellular interacting systems and show how these interactions can contribute to the derivation of a new class of chemotaxis models containing new terms to be compared with the classical ones.

We analyze the effect of interactions terms on the parabolic approximation and show how the classical chemotaxis equations and the news ones arise under suitable conditions on the kernel, and interactions operators. Moreover, our approach can be applied to derive more interesting chemotaxis models as a competitive system under chemotactic effects with non-local terms, and coupled chemotaxis-fluid models which use a two-scale kinetic-continuous framework.

The contents of this paper are of interest in the modeling of biological tissues, cancer angiogenesis phenomena [1, 23], pattern formation in populations of slime molds, swarming, and chemotaxis in different contexts [8, 9, 18, 20, 24, 31]. The guideline consists in start with microscopic models from kinetic theory and then derive macroscopic models by a micro–macro formulation. Subsequently, different variants of the Keller–Segel model are derived from the obtained macroscopic one by taking different scale regimes.

The presentation is organized as follows. Section 2. deals with the basic description of the class of equations of the kinetic theory that describe multicellular systems and the derivation of parabolic equations by using a kinetic–fluid formulation in the case of absence of biological interaction. In Section 3, we generalize the description to particles including interactions. Section 4 deals with the derivation of different variants of the Keller–Segel model (classical Keller–Segel model, the drift optimal Keller–Segel model, and a chemotaxis model with saturated chemotaxis flux, pressureless hyperbolic description (direct drift coupling), a competitive system under chemotactic effects with non-local terms), thought different macroscopic scalings. Section 5 shows that the above approach is specifically applied to derive a broad class of two-scales models of a coupled chemotaxis–fluid phenomena. Moreover, it is shown that this general approach technically leads to some models known in the literature corresponding to well defined assumptions on interactions at the scale of cells. Finally Section 6 proposes some research perspectives arising from conceivable applications of our approach to complex biological phenomena with special attention to growth and invasion phenomena and multiscale topics.

2. Linear Transport Models with Stochastic Velocity Jump Perturbation

2.1. The kinetic model

This section presents the derivation of macroscopic models, by micro-macro decomposition, of linear transport models of multicellular systems of a binary mixture of cells whose state, called *microscopic state*, is denoted by the variable (x, v), where $\{x, v\}$ are, respectively, position and velocity of the cell. The collective description is encoded in the statistical distribution functions $f_i = f_i(t, x, v)$, for $i = 1, 2$, which is called generalized distribution function. Weighted moments provide, under suitable integrability properties, the calculation of macroscopic variables. More precisely, let us consider the following class of equations:

$$\begin{cases} \big(\partial_t + v \cdot \nabla_x\big) f_1 = \nu_1\, \mathcal{T}_1(f_1), \\[2ex] \big(\partial_t + v \cdot \nabla_x\big) f_2 = \nu_2 \mathcal{T}_2(f_2), \end{cases} \tag{2.1}$$

where $f = \{f_1, f_2\}$, while the operator $\mathcal{T}_i(f_i)$ models the dynamics of biological organisms by a velocity-jump process:

$$\mathcal{T}_i(f) = \int_V \Big[T_i(v, v^*) f(t, x, v^*) - T_i(v^*, v) f(t, x, v) \Big]\, dv^*, \quad i = 1, 2, \tag{2.2}$$

where $T_i(v, v^*)$ is the probability kernel for the new velocity $v \in V$ assuming that the previous velocity was v^*. The operators T_i may depend on f_1 and f_2; in fact, we will assume that T_1 depends on the population f_2. The set of possible velocities is denoted by $V \subset \mathbb{R}^d$, assumed to be bounded and radial symmetric. Finally, ν_1 and ν_2 represent the interaction rates of the mechanical interactions.

2.2. The parabolic–parabolic approximation

Different scenarios that can appear when dealing with parabolic approximation for both populations are introduced in this subsection. These approximations depend on the scaling choice for the mechanical constants. First the basis of the kinetic approach to this microscopic model is given; then, based on the decomposition of micro–macro of the solutions, different approximation cases can be deduced.

The aim of this section consists in the derivation of macroscopic models (as for example those of chemotaxis) from the kinetic model (2.1). These macroscopic equations can be obtained in the regime $\nu_1, \nu_2 \to +\infty$. After a dimensionless of the system is obtained, see [4], a small parameter ε can be chosen such that

$$\nu_1 = \frac{1}{\varepsilon^p}, \qquad \nu_2 = \frac{1}{\varepsilon^q}, \qquad p, q \geq 1.$$

Then, the model (2.1) can be written as follows:

$$\begin{cases} \big(\varepsilon \partial_t + v \cdot \nabla_x\big) f_1^\varepsilon = \frac{1}{\varepsilon^p} \mathcal{T}_1[{f_2}^\varepsilon](f_1^\varepsilon), \\ \big(\varepsilon \partial_t + v \cdot \nabla_x\big) f_2^\varepsilon = \frac{1}{\varepsilon^q} \mathcal{T}_2(f_2^\varepsilon), \end{cases} \tag{2.3}$$

where the turning operator $\mathcal{T}_1[f_2]$ is supposed to be decomposed as follows:

$$\mathcal{T}_1[f_2](g) = \mathcal{T}_1^0(g) + \varepsilon \mathcal{T}_1^1[f_2](g), \tag{2.4}$$

where $\mathcal{T}_1^i$ for $i = 0, 1$ is given by

$$\mathcal{T}_1^i(g) = \int_V \Big[T_1^i g(t, x, v^*) - T_1^{i*} g(t, x, v) \Big] dv^*, \tag{2.5}$$

with $T_1^{i*} = T_1^i(v^*, v)$.

The dependence on f_2 of the operator $T_1[f_2]$ stems from T_1^1, while we suppose that $\mathcal{T}_1^0$ is independent on f_2.

Let us now first state some detailed assumptions on the turning operator $\mathcal{T}_i (i = 1, 2)$.

Assumption 2.1. *We assume that the turning operators $\mathcal{T}_1$ and $\mathcal{T}_2$ satisfy*

$$\int_V \mathcal{T}_1(g) dv = \int_V \mathcal{T}_1^0(g) dv = \int_V \mathcal{T}_1^1[f_2](g) dv = \int_V \mathcal{T}_2(g) dv = 0. \tag{2.6}$$

Some definitions and further assumptions are necessary to develop the asymptotic analysis leading to the derivation of macroscopic models.

Assumption 2.2. *There exists a bounded velocity distribution $M_i(v) > 0$, $i = 1, 2$ independent of t, x, such that the detailed balance*

$$T_1^0(v, v^*) M_1(v^*) = T_1^0(v^*, v) M_1(v), \tag{2.7}$$

and

$$T_2(v, v^*) M_2(v^*) = T_2(v^*, v) M_2(v) \tag{2.8}$$

holds. Moreover, the flow produced by these equilibrium distributions vanishes, and M_i are normalized, i.e.

$$\int_V v\, M_i(v) dv = 0, \quad \int_V M_i(v) dv = 1, \quad i = 1, 2. \tag{2.9}$$

In addition, the kernels $T_1^0(v,v^*)$ *and* $T_2(v,v^*)$ *are bounded, and there exists a constant* $\sigma_i > 0$, $i = 1,2$, *such that*

$$T_1^0(v,v^*) \geq \sigma_1 M_1(v), \quad T_2(v,v^*) \geq \sigma_2 M_2(v), \tag{2.10}$$

for all $(v,v^*) \in V \times V$, $x \in \Omega$ *and* $t > 0$.

Let now $L_1 = \mathcal{T}_1^0$ and $L_2 = \mathcal{T}_2$. Technical calculations, see [2], namely by integration over v, interchanging v by v^*, and using (2.7)-(2.8), yields the following equality:

$$\begin{aligned} \int_V L_i(g)\frac{h(v)}{M_i(v)}\,dv &= \frac{1}{2}\int_V\int_V \Psi[M_i]\left(\frac{g(v^*)}{M_i(v^*)} - \frac{g(v)}{M_i(v)}\right) \\ &\quad \times \left(\frac{h(v)}{M_i(v)} - \frac{h(v^*)}{M_i(v^*)}\right)dv\,dv^*, \end{aligned} \tag{2.11}$$

where

$$\Psi[M_1] = \frac{1}{2}\big(T_1^0(v,v_*)M_1(v_*) + T_1^0(v_*,v)M_1(v)\big),$$
$$\Psi[M_2] = \frac{1}{2}\big(T_2(v,v_*)M_2(v_*) + T_2(v_*,v)M_2(v)\big).$$

In particular Eq.(2.11) shows that the operators L_i, $(i = 1,2)$ are a self-adjoint and the following equality:

$$-\int_V L_i(h)\frac{h(v)}{M_i(v)}\,dv = \frac{1}{2}\int_V\int_V \Psi[M_i]\left(\frac{h(v)}{M_i(v)} - \frac{h(v^*)}{M_i(v^*)}\right)^2 dv\,dv^* \geq 0, \tag{2.12}$$

holds true.

Moreover, for $\int_V h(v)\,dv = 0$, Eq.(2.12) and the estimate (2.10) yield the following inequality:

$$\begin{aligned} -\int_V L_i(h)\frac{h(v)}{M_i(v)}\,dv &\geq \frac{\sigma_i}{2}\int_V\int_V M_i(v)M_i(v^*)\left(\frac{h(v)}{M_i(v)} - \frac{h(v^*)}{M_i(v^*)}\right)^2 dv\,dv^* \\ &\geq \sigma_i\int_V \frac{h^2(v)}{M_i(v)}\,dv, \quad i = 1,2, \end{aligned} \tag{2.13}$$

which shows that L_i is a Fredholm operator in the space $L^2(V, \frac{dv}{M_i(v)})$. Therefore, the following result defines the properties of the operator L_i:

Lemma 1. *Suppose that Assumptions 2.2 hold. Then, the following properties of the operators* L_1 *and* L_2 *hold true:*

i) The operator L_i *is self-adjoint in the space* $L^2\left(V, \dfrac{dv}{M_i}\right)$.

ii) For $f \in L^2$, *the equation* $L_i(g) = f$, $i = 1,2$, *has a unique solution* $g \in L^2\left(V, \dfrac{dv}{M_i}\right)$, *which satisfies*

$$\int_V g(v)\,dv = 0 \quad \textit{if and only if} \quad \int_V f(v)\,dv = 0.$$

iii) The equation $L_i(g) = v\, M_i(v)$, $i = 1, 2$, has a unique solution that we call $\theta_i(v)$.

iv) The kernel of L_i is $N(L_i) = vect(M_i(v))$, i=1,2.

2.3. A kinetic-fluid formulation

In this subsection, we show that the kinetic equation (2.3) can be equivalently written as a system coupling a hydrodynamic part with a kinetic part of the distribution functions.

In what follows the integral with respect to the variable v will be denoted by $\langle . \rangle$, and let

$$n(t,x) = \int_V f_1 dv, \quad S(t,x) = \int_V f_2 dv,$$

and $f = (f_1, f_2)$ be a solution of (2.3). We compose f as follows

$$f_1 = M_1(v)n + \varepsilon g_1, \quad f_2 = M_2(v)S + \varepsilon g_2, \tag{2.14}$$

then $\langle g_i \rangle = 0, i = 1, 2,$ and one has:

$$\begin{aligned} \partial_t(M_1 n) \ &+ \ \varepsilon \partial_t g_1 + \frac{1}{\varepsilon} v M_1 \cdot \nabla_x n + v \cdot \nabla_x g_1 = \frac{1}{\varepsilon^p} \mathcal{T}_1^0(g_1) \\ &+ \ \frac{1}{\varepsilon^p} \mathcal{T}_1^1(f_2)(M_1(v)n) + \frac{1}{\varepsilon^{p-1}} \mathcal{T}_1^1(f_2)(g_1), \end{aligned} \tag{2.15}$$

and

$$\partial_t(M_2 S) + \varepsilon \partial_t g_2 + \frac{1}{\varepsilon} v M_2 \cdot \nabla_x S + v \cdot \nabla_x g_2 = \frac{1}{\varepsilon^q} \mathcal{T}_2(g_2). \tag{2.16}$$

Now, we use a projection technique to separate the macroscopic and microscopic quantities $n(t,x)$, $S(t,x)$ and $g_1(t,x,v)$, $g_2(t,x,v)$. Moreover, let P_{M_1}, P_{M_2} denote respectively the orthogonal projection onto $N(\mathcal{T}_1^0)$, and $N(\mathcal{T}_2)$. Then

$$P_{M_i}(h) = \langle h \rangle M_i, \quad i = 1, 2 \quad \text{for any} \quad h \in L^2(V, \frac{dv}{M_i(v)}),$$

so that one has the following:

Lemma 2. *One has the following properties for the projection P_{M_i}, $i = 1, 2$:*

$$(I - P_{M_1})(M_1 n) = (I - P_{M_2})(M_2 S) = P_{M_i}(g_i) = 0, \quad i = 1, 2,$$

$$\begin{gathered} (I - P_{M_1})(v M_1 \cdot \nabla_x n) = v M_1 \cdot \nabla_x n, \\ (I - P_{M_2})(v M_2 \cdot \nabla_x S) = v M_2 \cdot \nabla_x S, \\ (I - P_{M_1})(\mathcal{T}_1^1(f_2)(M(v)n) = \mathcal{T}_1^1(f_2)(M(v)n), \\ (I - P_{M_1})(\mathcal{T}_1^1(f_2)(g)) = \mathcal{T}_1^1(f_2)(g), \\ (I - P_{M_2})(\mathcal{T}_2(g)) = \mathcal{T}_2(g). \end{gathered}$$

Proof. The firsts equality are trivial since $P_{M_i}(M_i) = M_i$, and $\langle g_i \rangle = 0$. As the flux produced by M_i is zero then

$$(I - P_{M_1})(vM_1 \cdot \nabla_x n) = vM_1 \cdot \nabla_x n,$$

and

$$(I - P_{M_2})(vM_2 \cdot \nabla_x S) = vM_2 \cdot \nabla_x S.$$

Using (2.6), one deduce that

$$P_{M_1}(\mathcal{T}_1^1(f_2)(h)) = P_{M_2}(\mathcal{T}_2(h)) = 0,$$

for any $h \in L^2(V, \frac{dv}{M_i})$, and then the last three equality are proved.

Inserting the operators $I - P_{M_1}$, and $I - P_{M_2}$ respectively into Eq.(2.15), Eq.(2.16) and using the above lemma, yields:

$$\begin{aligned} \varepsilon\partial_t g_1 &+ \frac{1}{\varepsilon} vM_1 \cdot \nabla_x n + (I - P_{M_1})(v \cdot \nabla_x g_1) = \frac{1}{\varepsilon^p}\mathcal{T}_1^0(g_1) \\ &+ \frac{1}{\varepsilon^p}\mathcal{T}_1^1(f_2)(M_1(v)n) + \frac{1}{\varepsilon^{p-1}}\mathcal{T}_1^1(f_2)(g_1), \end{aligned} \tag{2.17}$$

$$\varepsilon\partial_t g_2 + \frac{1}{\varepsilon} vM_2 \cdot \nabla_x S + (I - P_{M_2})(v \cdot \nabla_x g_2) = \frac{1}{\varepsilon^q}\mathcal{T}_2(g_2). \tag{2.18}$$

Integrating (2.15), (2.16) over v, using (2.6), yields:

$$\partial_t n + \langle v \cdot \nabla_x g_1 \rangle = 0, \tag{2.19}$$

$$\partial_t S + \langle v \cdot \nabla_x g_2 \rangle = 0. \tag{2.20}$$

Then the micro-macro formulation finally reads

$$\begin{cases} \varepsilon\partial_t g_1 + \frac{1}{\varepsilon} vM_1 \cdot \nabla_x n + (I - P_{M_1})(v \cdot \nabla_x g_1) = \\ \frac{1}{\varepsilon^p}\mathcal{T}_1^0(g_1) + \frac{1}{\varepsilon^p}\mathcal{T}_1^1(f_2)(M_1(v)n) + \frac{1}{\varepsilon^{p-1}}\mathcal{T}_1^1(f_2)(g_1), \\ \partial_t n + \langle v \cdot \nabla_x g_1 \rangle = 0, \\ \varepsilon\partial_t g_2 + \frac{1}{\varepsilon} vM_2 \cdot \nabla_x S + (I - P_{M_2})(v \cdot \nabla_x g_2) = \frac{1}{\varepsilon^q}\mathcal{T}_2(g_2), \\ \partial_t S + \langle v \cdot \nabla_x g_2 \rangle = 0. \end{cases} \tag{2.21}$$

Equations (2.21) represent the micro-macro formulation of the kinetic equation (2.3). The following proposition shows that this formulation is indeed equivalent to the kinetic equation (2.3).

Proposition 3. *i) Let* $f = (f_1, f_2)$ *be a solution of the kinetic equation (2.3). Then the functions* (n, g_1, S, g_2)*, where* $n = \langle f_1 \rangle$*,* $S = \langle f_2 \rangle$ *and* $g_1 = \frac{1}{\varepsilon}(f_1 - M_1 n)$*,* $g_2 = \frac{1}{\varepsilon}(f_2 - M_2 S)$ *is a solution to a coupled system (2.21) with the associated initial data.*

$$n(t = 0) = n_0 = \langle f_{10} \rangle, \quad g_1(t = 0) = g_{10} = \frac{1}{\varepsilon}(f_{10} - M_1 n_0), \tag{2.22}$$

$$S(t=0) = S_0 = \langle f_{20} \rangle, \quad g_2(t=0) = g_{20} = \frac{1}{\varepsilon}(f_{20} - M_2 S_0). \tag{2.23}$$

ii) Conversely, if (n, g_1, S, g_2) *satisfies system (2.21) with initial data* $(n_0, g_{10}, S_0, g_{20})$ *such that* $\langle g_{10} \rangle = \langle g_{20} \rangle = 0$*, then* $f_1 = M_1 n + \varepsilon g_1$*,* $f_2 = M_2 S + \varepsilon g_2$ *is a solution to kinetic model (2.3) with initial data* $f_{10} = M_1 n_0 + \varepsilon g_{10}$*,* $f_{20} = M_2 S_0 + \varepsilon g_{20}$ *and we have* $n = \langle f_1 \rangle$*,* $S = \langle f_2 \rangle$ *and* $\langle g_1 \rangle = \langle g_2 \rangle = 0$*.*

Proof. The proof of i) is already detailed above. For the proof ii) consider (n, g_1, S, g_2) solution of (2.21). Setting $f_1 = M_1 n + \varepsilon g_1$, $f_2 = M_2 S + \varepsilon g_2$, it can be shown that $f = (f_1, f_2)$ is a solution of kinetic model (2.3). From (2.21), one has

$$\partial_t f_1 - M_1(v)\partial_t n + \frac{1}{\varepsilon} v M_1 \cdot \nabla_x n + v \cdot \nabla_x g_1 - P_{M_1}(v \cdot \nabla_x g_1) = \frac{1}{\varepsilon^p} \mathcal{T}_1^0(g_1)$$

$$+ \frac{1}{\varepsilon^p} \mathcal{T}_1^1[f_2](M_1(v)n) + \frac{1}{\varepsilon^{p-1}} \mathcal{T}_1^1[f_2](g_1).$$

Therefore

$$\partial_t f_1 - M_1(v)\partial_t n + \frac{1}{\varepsilon} v \cdot \nabla_x f_1 - M_1(v)\langle v \cdot \nabla_x g_1 \rangle = \frac{1}{\varepsilon^p} \mathcal{T}_1[f_2](f_1).$$

Using Eq.(2.19) yields the first equation for f_1 in (2.3), while the property $\langle g_1 \rangle = 0$ is obtained by noting that

$$\langle (I - P_{M_1})(v \cdot \nabla_x g_1) \rangle = 0.$$

Then integrating Eq.(2.17) over v, yields

$$\partial_t \langle g_1 \rangle = 0,$$

which gives the result by using the property of the initial data.

The same techniques applied to Eq.(2.18) for the second population completes the proof of Proposition.

In order to develop asymptotic analysis of Eqs.(2.3), one needs additional assumptions on the operator $\mathcal{T}_1^1$.

Assumption 2.3. *We assume that the turning operators* $\mathcal{T}_1^1$ *satisfy the following asymptotic behavior:*

$$\mathcal{T}_1^1[M_2(v)S + \varepsilon g_2] = \mathcal{T}_1^1[M_2(v)S] + O(\varepsilon), \quad as \quad \varepsilon \longrightarrow 0. \tag{2.24}$$

2.4. Derivation of a general macroscopic models

Here, we rapidly show that the micro-macro formulation (2.21) of the kinetic equation (2.3) allows to obtain very easily the corresponding macroscopic models as ε *goes to* 0*, without using the Hilbert expansion. Indeed, Eqs.(2.21) give*

$$\mathcal{T}_1^0(g_1) = \varepsilon^{p-1} v M_1 \cdot \nabla_x n - \mathcal{T}_1^1[f_2](M_1(v)n) + O(\varepsilon),$$

$$\mathcal{T}_2(g_2) = \varepsilon^{q-1} v M_2 \cdot \nabla_x S + O(\varepsilon^q).$$

As

$$\langle v M_1 \rangle = \langle v M_2 \rangle = \langle \mathcal{T}_1^1[f_2](M_1(v)n) \rangle = 0,$$

then $\mathcal{T}_1^0$, and $\mathcal{T}_2$ are invertible and one obtains:

$$g_1 = \varepsilon^{p-1} (\mathcal{T}_1^0)^{-1}(v M_1 \cdot \nabla_x n) - (\mathcal{T}_1^0)^{-1}(\mathcal{T}_1^1[f_2](M_1(v)n)) + O(\varepsilon), \tag{2.25}$$

$$g_2 = \varepsilon^{q-1} (\mathcal{T}_2)^{-1}(v M_2 \cdot \nabla_x S) + O(\varepsilon^q). \tag{2.26}$$

Using (2.24), and inserting (2.25)-(2.26) into (2.21), yields the following macroscopic models:

$$\begin{cases} \partial_t n + \varepsilon^{p-1} \left\langle v \cdot \nabla_x (\mathcal{T}_1^0)^{-1}(v M_1 \cdot \nabla_x n) \right\rangle \\ \\ - \left\langle v \cdot \nabla_x (\mathcal{T}_1^0)^{-1}(\mathcal{T}_1^1[M_2(v)S](M_1(v)n)) \right\rangle + O(\varepsilon) = 0, \\ \\ \partial_t S + \varepsilon^{q-1} \left\langle v \cdot \nabla_x (\mathcal{T}_2)^{-1}(v M_2 \cdot \nabla_x S) \right\rangle + O(\varepsilon^q) = 0. \end{cases} \tag{2.27}$$

Lemma 4. *Suppose that Assumptions 2.2 hold for $\mathcal{T}_1^0$, and $\mathcal{T}_2$. Then One has the following identities:*

$$\Big\langle v \cdot \nabla_x (\mathcal{T}_1^0)^{-1}(v M_1 \cdot \nabla_x n) \Big\rangle = div_x \Big(\langle v \otimes \theta_1(v) \rangle \cdot \nabla_x n \Big),$$

$$\Big\langle v \cdot \nabla_x (\mathcal{T}_2)^{-1}(v M_2 \cdot \nabla_x S) \Big\rangle = div_x \Big(\langle v \otimes \theta_2(v) \rangle \cdot \nabla_x S \Big),$$

$$\Big\langle v \cdot \nabla_x (\mathcal{T}_1^0)^{-1}(\mathcal{T}_1^1[M_2(v)S](M_1(v)n)) \Big\rangle = div_x \left\langle \frac{\theta_1(v)}{M_1(v)} n \mathcal{T}_1^1[M_2(v)S](M_1(v)) \right\rangle,$$

where θ_1 and θ_2 are given in Lemma 1.

Proof. *For the first and second identities, we use Lemma 1. As $\mathcal{T}_1^0$ is a self adjoint operator in $L^2(\frac{dv}{M_1(v)})$, one has*

$$\begin{aligned} &\left\langle v \cdot \nabla_x (\mathcal{T}_1^0)^{-1}(\mathcal{T}_1^1[M_2(v)S](M_1(v)n)) \right\rangle \\ &\quad = \left\langle v M_1(v) \cdot \frac{\nabla_x}{M_1(v)} (\mathcal{T}_1^0)^{-1}(\mathcal{T}_1^1[M_2(v)S](M_1(v)n)) \right\rangle \\ &\quad = \left\langle \mathcal{T}_0^1(\theta_1(v)) \cdot \frac{\nabla_x}{M_1(v)} (\mathcal{T}_1^0)^{-1}(\mathcal{T}_1^1[M_2(v)S](M_1(v)n))) \right\rangle \\ &\quad = div_x \left\langle \frac{\theta_1(v)}{M_1(v)} n \mathcal{T}_1^1[M_2(v)S](M_1(v)) \right\rangle. \end{aligned}$$

This completes the proof.

One has the following result:

Theorem 5. *Let* $f = (f_1, f_2)$ *be a solution to the kinetic equation (2.3) such that, when it is written according to formula (2.14), Assumptions 2.1-2.2 hold. Then the macroscopic variables* (n, S)*, where* $n = \langle f_1 \rangle$ *and* $S = \langle f_2 \rangle$*, are solution to the coupled macroscopic system:*

$$\begin{cases} \partial_t n + div_x \left(n\alpha(S) - \varepsilon^{p-1} D_n \cdot \nabla_x n \right) + O(\varepsilon) = 0, \\ \\ \partial_t S - \varepsilon^{q-1} div_x (D_S \cdot \nabla_x S) + O(\varepsilon^q) = 0, \end{cases} \tag{2.28}$$

with initial data given by:

$$n(t=0) = n_0 = \langle f_{10} \rangle, \quad S(t=0) = S_0 = \langle f_{20} \rangle, \tag{2.29}$$

where $\alpha(S)$ *is given by*

$$\alpha(S) = -\int_V \frac{\theta_1(v)}{M_1(v)} \mathcal{T}_1^1(M_2(v)S)(M_1(v))dv, \tag{2.30}$$

and where the diffusion coefficients D_n *and* D_S *are symmetric, positive definite, and given by*

$$D_n = -\int_V v \otimes \theta_1(v)dv, \quad D_S = -\int_V v \otimes \theta_2(v)dv. \tag{2.31}$$

Proof. Using Proposition 3, Lemma 4, and (2.27), yields the macroscopic models (2.28)-(2.31). In order to verify that D_n and D_S are symmetric and positive defined, let us consider $x \in \mathbb{R}^d$. Then, from (2.31) and by using (2.13), one has

$$\begin{aligned} D_n x \cdot x &= -\int_V (\theta_1(v) \cdot x)(v \cdot x)\, dv = -\int_V \mathcal{T}_1^0(\theta_1(v) \cdot x)(\theta_1(v) \cdot x) \frac{dv}{M_1(v)} \\ &\geq \sigma_1 \int_V (\theta_1(v) \cdot x)^2 \frac{dv}{M_1(v)}, \end{aligned}$$

and

$$\begin{aligned} D_S x \cdot x &= -\int_V \mathcal{T}_2(\theta_2(v) \cdot x)(\theta_2(v) \cdot x) \frac{dv}{M_2(v)} \\ &\geq \sigma_2 \int_V (\theta_2(v) \cdot x)^2 \frac{dv}{M_2(v)}. \end{aligned}$$

If $D_n x \cdot x$ were identically equal to zero for $x \neq 0$, then $v \cdot x$ would be zero for all $v \in V$, which is impossible due to the spherical symmetry of V. The symmetry of D_n is an immediate consequence of that $\mathcal{T}_0^1$ is self-adjoint with respect to the scalar product in $L^2(V, \frac{dv}{M_1(v)})$. This completes the proof.

Remark 6. *In general* D_n *and* D_S *are not isotropic (there are not scalar factor of the identity matrix). An example where the tensors* D_n *and* D_S *are isotropic will be given in Sec 4. The approach we have developed is quite general. Some more specific examples are reported in Section 4.*

Now, we extend the kinetic-fluid formulation developed in Section 3 to models with death/birth process, and we show after some assumptions on the interactions operators that a new class of macroscopic models incorporating new terms can be obtained. Finally, several examples motivated in the choice of the transport and interactions operators involved in our general kinetic model are reported in Sections 4 and 5.

3. Binary mixture with biological interactions

Let us consider a binary mixture of cells where the output of interactions includes birth-death processes, adding

$$\left(\frac{\partial f}{\partial t}\right)_{bd} = (G_1(f_1, f_2, v), G_2(f_1, f_2, v))$$

to the right hand side of (2.3), thus we consider the following class of equations modeling the dynamics of $f = (f_1, f_2)$*:*

$$\begin{cases} \big(\varepsilon\partial_t + v\cdot\nabla_x\big) f_1^\varepsilon = \frac{1}{\varepsilon^p}\mathcal{T}_1[f_2^\varepsilon](f_1^\varepsilon) + G_1(f_1^\varepsilon, f_2^\varepsilon, v), \\ \\ \big(\varepsilon\partial_t + v\cdot\nabla_x\big) f_2^\varepsilon = \frac{1}{\varepsilon^q}\mathcal{T}_2(f_2^\varepsilon) + G_2(f_1^\varepsilon, f_2^\varepsilon, v), \end{cases} \tag{3.1}$$

where the operator $\mathcal{T}_i$ *was already described in Section 2. Moreover the operators* $G_i, i = 1, 2,$ *which describe the gain–loss balance of cells, chemoattractant, molecules, etc., are supposed to satisfy the following:*

Assumptions 3.1.*We assume that the operators* G_i *satisfy the following:*

$$G_i(f_1, f_2, v) = G_{i1}(f_1, f_2, v) + \varepsilon G_{i2}(f_1, f_2, v), \quad i = 1, 2, \tag{3.2}$$

where

$$\int_V G_{i1}(f_1, f_2, v)dv = 0, \quad i = 1, 2, \tag{3.3}$$

moreover G_{i1} *is assumed to satisfy the following: when* $\varepsilon \to 0$*:*

$$G_{ij}(M_1(v)n + \varepsilon g_1, M_2(v)S + \varepsilon g_2, v) = G_{ij}(M_1(v)n, M_2(v)S, v) + O(\varepsilon), \quad i, j = 1, 2. \tag{3.4}$$

3.1. Micro-macro decomposition, and derivation of a general macroscopic model

A development of micro-macro decomposition is treated in the following thus obtaining different macro-scale models. Let us now consider, referring to Eqs. (3.1), the equations for g_1, g_2*, and for* the first moments n, S, which, instead of (2.21), the micro-macro formulation reads:

$$\begin{cases} \varepsilon\partial_t g_1 + \frac{1}{\varepsilon} v M_1 \cdot \nabla_x n + (I - P_{M_1})(v \cdot \nabla_x g_1) = \frac{1}{\varepsilon^p} \mathcal{T}_1^0(g_1) \\ \qquad + \dfrac{1}{\varepsilon^p} \mathcal{T}_1^1[f_2](M_1(v)n) + \dfrac{1}{\varepsilon^{p-1}} \mathcal{T}_1^1[f_2](g_1) \\ \qquad + \dfrac{1}{\varepsilon} G_{11}(f_1, f_2, v) + (I - P_{M_1}) G_{12}(f_1, f_2, v), \\ \partial_t n + \langle v \cdot \nabla_x g_1 \rangle = \langle G_{12}(f_1, f_2, v) \rangle, \\ \varepsilon\partial_t g_2 + \frac{1}{\varepsilon} v M_2 \cdot \nabla_x S + (I - P_{M_2})(v \cdot \nabla_x g_2) = \frac{1}{\varepsilon^q} \mathcal{T}_2(g_2) \\ \qquad + \dfrac{1}{\varepsilon} G_{21}(f_1, f_2, v) + (I - P_{M_2}) G_{22}(f_1, f_2, v), \\ \partial_t S + \langle v \cdot \nabla_x g_2 \rangle = \langle G_{22}(f_1, f_2, v) \rangle. \end{cases} \tag{3.5}$$

Using (3.4), the following equations for g_1 and g_2 can be obtained from (3.5):

$$\begin{aligned} \varepsilon\partial_t g_1 &+ \frac{1}{\varepsilon} v M_1 \cdot \nabla_x n + (I - P_{M_1})(v \cdot \nabla_x g_1) = \frac{1}{\varepsilon^p} \mathcal{T}_1^0(g_1) \\ &+ \frac{1}{\varepsilon^p} \mathcal{T}_1^1[f_2](M_1(v)n) + \frac{1}{\varepsilon^{p-1}} \mathcal{T}_1^1[f_2](g_1) \\ &+ \frac{1}{\varepsilon} G_{11}(M_1 n, M_2 S, v) + (I - P_{M_1}) G_{12}(f_1, f_2, v) + O(1), \end{aligned} \tag{3.6}$$

and

$$\begin{aligned} \varepsilon\partial_t g_2 &+ \frac{1}{\varepsilon} v M_2 \cdot \nabla_x S + (I - P_{M_2})(v \cdot \nabla_x g_2) = \frac{1}{\varepsilon^q} \mathcal{T}_2(g_2) \\ &+ \frac{1}{\varepsilon} G_{21}(M_1 n, M_2 S, v) + (I - P_{M_2}) G_{22}(f_1, f_2, v) + O(1). \end{aligned} \tag{3.7}$$

Then using (2.6), (3.3), and (3.6)-(3.7) yields the following:

$$\begin{aligned} g_1 &= \varepsilon^{p-1} (\mathcal{T}_1^0)^{-1} (v M_1 \cdot \nabla_x n) - (\mathcal{T}_1^0)^{-1} (\mathcal{T}_1^1(f_2)(M_1(v)n)) \\ &- \varepsilon^{p-1} (\mathcal{T}_1^0)^{-1} (G_{11}(M_1 n, M_2 S), v) + O(\varepsilon), \end{aligned} \tag{3.8}$$

and

$$g_2 = \varepsilon^{q-1} (\mathcal{T}_2)^{-1} (v M_2 \cdot \nabla_x S) - \varepsilon^{q-1} (\mathcal{T}_2)^{-1} (G_{21}(M_1 n, M_2 S, v)) + O(\varepsilon). \tag{3.9}$$

Inserting (3.8), and (3.9) into (3.5), yields the following nonlinear coupled macro-scale models:

$$\begin{cases} \partial_t n + \varepsilon^{p-1} \left\langle v \cdot \nabla_x (\mathcal{T}_1^0)^{-1} (v M_1 \cdot \nabla_x n) \right\rangle - \left\langle v \cdot \nabla_x (\mathcal{T}_1^0)^{-1} (\mathcal{T}_1^1 [M_2(v) S](M_1(v) n)) \right\rangle \\ -\varepsilon^{p-1} \left\langle v \cdot \nabla_x (\mathcal{T}_1^0)^{-1} (G_{11}(M_1 n, M_2 S, v)) \right\rangle = \langle G_{12}(M_1 n, M_2 S, v) \rangle + O(\varepsilon), \\ \partial_t S + \varepsilon^{q-1} \left\langle v \cdot \nabla_x (\mathcal{T}_2)^{-1} (v M_2 \cdot \nabla_x S) \right\rangle \\ -\varepsilon^{q-1} \left\langle v \cdot \nabla_x (\mathcal{T}_2)^{-1} (G_{21}(M_1 n, M_2 S, v)) \right\rangle = \left\langle G_{22}(M_1 n, M_2 S, v) \right\rangle + O(\varepsilon). \end{cases} \tag{3.10}$$

Now using the equality

$$\left\langle v \cdot \nabla_x (\mathcal{T}_1^0)^{-1} (G_{i1}(M_1 n, M_2 S)) \right\rangle = div_x \left\langle \frac{\theta_i(v)}{M_i(v)} G_{i1}(M_1 n, M_2 S, v) \right\rangle, \quad i = 1, 2,$$

and Lemma 4, yields the following macro-scale models:

$$\begin{cases} \partial_t n + div_x \left(n\alpha(S) + \varepsilon^{p-1} (\Gamma(n, S) - D_n \cdot \nabla_x n) \right) - H_1(n, S) + O(\varepsilon) = 0, \\ \partial_t S + \varepsilon^{q-1} div_x (\beta(n, S) - D_S \cdot \nabla_x S) - H_2(n, S) + O(\varepsilon) = 0, \end{cases} \tag{3.11}$$

where D_n, D_S, $\alpha(S)$ *are given respectively by (2.31), and (2.30), and* $\Gamma(n, S)$, $\beta(n, S)$, $H_1(n, S)$, *and* $H_2(n, S)$ *are given by the following:*

$$\Gamma(n, S) = -\int_V \frac{\theta_1(v)}{M_1(v)} G_{11}(M_1 n, M_2 S, v) dv, \tag{3.12}$$

$$\beta(n, S) = -\int_V \frac{\theta_2(v)}{M_2(v)} G_{21}(M_1 n, M_2 S, v) dv, \tag{3.13}$$

$$H_1(n, S) = \int_V G_{12}(M_1 n, M_2 S, v) dv, \quad H_2(n, S) = \int_V G_{22}(M_1 n, M_2 S, v) dv. \tag{3.14}$$

Remark 7. *1. The approach we have developed above is quite general, while more specific examples can be given. In particular, a suitable choice of the turning operators* T_1^0, T_1^1, T_2, *and* $G_{ij}, i, j = 1, 2$ *allows us to recover the Keller-Segel, chemotaxis model, models describing the evolution of a population under chemotactic effects with non-local reaction terms, pressureless hyperbolic description (direct drift coupling), and models for optimal drift following the chemoattractant.*
2. Models (3.11)-(3.14) differ from those obtained from a classical chemotaxis models by the terms $div_x \Gamma$, *and* $div_x \beta$. *These terms are very important to integrate in the modeling approach, in detail we will develop a new mesoscopic modelling approach for a coupled chemotaxis-fluid incorporating these terms which will be analysed at the end of the paper.*

In the next examples some nonlinear macro-scale models are derived based on appropriate assumptions on a relaxation properties of the turning operators T_1^0 *and* T_2.

4. Examples

4.1. Examples for linear turning kernels

Specific models for turning kernels and compute explicit formulas for the macroscopic transport coefficients are analysed in this subsection.

4.1.1. Example I: A general model for kernels with time relaxation

Let us first consider the following task for the probability kernels:

$$T_1^0(v,v^*) = \sigma_1 M_1(v), \qquad T_2(v,v^*) = \sigma_2 M_2(v), \quad \sigma_1,\ \sigma_2 > 0. \tag{4.1}$$

Consequently, the leading turning operators $\mathcal{T}_0^1$ *and* $\mathcal{T}_2$ *become relaxation operators:*

$$\mathcal{T}_1^0(g) = -\sigma_1\Big(g - \langle g\rangle M_1\Big), \qquad \mathcal{T}_2(g) = -\sigma_2\Big(g - \langle g\rangle M_2\Big). \tag{4.2}$$

In particular, θ_1 *and* θ_2 *are given by*

$$\theta_1(v) = -\frac{1}{\sigma_1}\, vM_1(v), \qquad \theta_2(v) = -\frac{1}{\sigma_2}\, vM_2(v).$$

Moreover α, Γ, *and* β *given by (2.30), (3.12), and (3.13) become:*

$$\alpha(S) = \frac{1}{\sigma_1}\int_V v\mathcal{T}_1^1[M_2 S](M_1)(v), \tag{4.3}$$

$$\Gamma(n,S) = \int_V \frac{v}{\sigma_1} G_{11}(M_1 n, M_2 S, v)dv, \quad \beta(n,S) = \int_V \frac{v}{\sigma_2} G_{21}(M_1 n, M_2 S, v)dv, \tag{4.4}$$

while the diffusion tensors D_n *and* D_S *are given by*

$$D_n = \frac{1}{\sigma_1}\int_V v\otimes vM_1(v)dv, \quad D_S = \frac{1}{\sigma_2}\int_V v\otimes vM_2(v)dv. \tag{4.5}$$

We will examine several forms for the dependence of the kernel on f_2 *and its gradient, some of which lead to the classical systems such as chemotaxis models.*

4.1.2. Example II: Some fundamentals of Chemotaxis

The relaxation kernels presented in Section 2, together with the choice

$$T_1^1[f_2] = K_{\frac{f_2}{M_2}}(v,v^*)\cdot\nabla_x \frac{f_2}{M_2}, \tag{4.6}$$

where $K_{\frac{f_2}{M_2}}(v,v^*)$ *is a vector valued function satisfying the following behavior*

$$K_{S+\varepsilon\frac{g_2}{M_2}} = K_S + O(\varepsilon), \quad as \quad \varepsilon\to 0. \tag{4.7}$$

Then T_1^1 satisfies (2.24), and leads to the model

$$\mathcal{T}_1^1[M_2S](M_1) = \delta(v,S)\cdot\nabla_x S,$$

where

$$\delta(v,S) = \int_V \Big(K_S(v,v^*)M_1(v^*) - K_S(v^*,v)M_1(v)\Big)dv^*.$$

Finally, the function $\alpha(S)$ in (4.3) is given by

$$\alpha(S) = \chi(S)\cdot\nabla_x S,$$

where the chemotactic sensitivity $\chi(S)$ is given by the matrix

$$\chi(S) = \frac{1}{\sigma_1}\int_V v\otimes\delta(v,S)dv. \tag{4.8}$$

Therefore, chemotaxis type models incorporating a new terms are obtained:

$$\begin{cases} \partial_t n + div_x\,(n\,\chi(S)\cdot\nabla_x S + \varepsilon^{p-1}(\Gamma(n,S) - D_n\cdot\nabla_x n)) \\ \qquad\qquad -H_1(n,S) + O(\varepsilon) = 0, \\ \partial_t S + \varepsilon^{q-1}div_x(\beta(n,S) - D_S\cdot\nabla_x S) - H_2(n,S) + O(\varepsilon) = 0. \end{cases} \tag{4.9}$$

4.1.3. Example III: Keller Segel models

Let $p = q = 1$, and $G_{11} = G_{21} = 0$, then $\Gamma(n,S) = \beta(n,S) = 0$, and then from (4.9) one has the following macro-scale type models up to ε:

$$\begin{cases} \partial_t n + div_x\,(n\,\chi(S)\cdot\nabla_x S - D_n\cdot\nabla_x n) - H_1(n,S) + O(\varepsilon) = 0, \\ \partial_t S - D_S\Delta S - H_2(n,S) + O(\varepsilon) = 0. \end{cases} \tag{4.10}$$

The role of the functions $H_1(n,S)$ and $H_2(n,S)$ in (4.10) consists in modelling the interaction between both quantities. For example, the Slime Mold Amebae produce themselves the chemoattractant when nourishment lacks [29]. These phenomena can be obtained from (3.1) by choosing:

$$G_{12} = 0, \quad G_{22}(f_1,f_2) = af_1 - bf_2, \quad a,b\geq 0.$$

Therefore, one has:

$$H_2(n,S) = \int_V G_{22}(M_1 n, M_2 S, v)dv = a\,n - b\,S,$$

while the macroscopic model (2.28) writes:

$$\begin{cases} \partial_t n + div_x\,(n\,\chi(S)\cdot\nabla_x S - D_n\cdot\nabla_x n) + O(\varepsilon) = 0, \\ \partial_t S - D_S\Delta S = an - bS + O(\varepsilon). \end{cases} \tag{4.11}$$

4.1.4. Example IV: On a competitive system under chemotactic effects with non-local terms

In this example we try to obtain a system of partial differential equations describing the evolution of a population under chemotactic effects with non-local reaction terms [34], [38]. This model extend the Parabolic Keller-Segel system by introducing non-local terms in the logistic growth factor. We denote by n the density of the population of living organisms which satisfies a parabolic equation with constant diffusion and chemotactic sensitivity χ. The equation presents a growth factor of logistic type defined in terms of the total mass of the population (the non-local term). If we denote the chemoattractant substance by S, the equation is as follows:

$$\begin{cases} \partial_t n + div_x\,(n\,\chi(S)\cdot\nabla_x S - D_n\cdot\nabla_x n) = n(a_0 + a_1 n - \frac{a_2}{|\Omega|}\int_\Omega n\,dx), \\ \\ \partial_t S - D_S\Delta S = n - S, \end{cases} \tag{4.12}$$

for a_0 and a_1 positive, $a_2 \in \mathbb{R}$. The coefficient a_0, sometimes also called Malthusian parameter, induces an exponential growth for low density populations. At the time that the population grows, the competitive effect of the local term $a_1 n$ becomes more influential. The non-local term $n\frac{a_2}{|\Omega|}\int_\Omega ndx$ describes the influence of the total mass of the species in the growth of the population.

Now consider the model (3.1)-(3.3), with

$$G_{12}(f_1,f_2,v) = f_1\left(a_0 + f_1\frac{a_1}{\int_V M_1^2 dv} - \frac{a_2}{\mid\Omega\mid}\int_\Omega ndx\right), \quad G_{22}(f_1,f_2,v) = f_1 - f_2,$$

with $n(t,x) = \int_V f_1(t,x,v)dv$. Therefore, one has:

$$H_1(n,S) = \int_V G_{12}(M_1 n, M_2 S, v)dv = n\left(a_0 + a_1 n - \frac{a_2}{\mid\Omega\mid}\int_\Omega ndx\right),$$

$$H_2(n,S) = \int_V G_{22}(M_1 n, M_2 S, v)dv = n - S,$$

and the macroscopic model (2.28) gives (4.12) up to ε.

4.1.5. Example V: Pressureless hyperbolic description (direct drift coupling)

In this example we try to obtain a model that preserves a drift term for the first population produced by the concentration gradient of the other population (think for example in chemical substance), but eliminating the diffusion effects.

Let now $p > 1, q = 1$, and $G_{21} = 0$, then $\beta(n,S) = 0$, and then from (4.9) one has the following macro-scale model:

$$\begin{cases} \partial_t n + div_x\,(n\,\chi(S)\cdot\nabla_x S) = H_1(n,S) + O(\varepsilon), \\ \\ \partial_t S - D_S\Delta S = H_2(n,S) + O(\varepsilon). \end{cases} \tag{4.13}$$

4.1.6. Example VI: Optimal drift following the chemoattractant (different regimes for the optimal drift)

More general one consider a regularization of the PKS model, which is based on a fundamental biological property of the chemotactic flux function-its boundedness (this feature is almost always lost in weakly nonlinear, small gradients expansions, underlying the derivation of most continuum models). To derive the modified system we replace the linear chemotactic flux $\chi n \nabla_x S$ *by a nonlinear saturated one,* $\chi n Q(\nabla_x S)$*, which is proportional to the magnitude of the chemoattractant gradient only when the latter is small and is bounded when the chemoattractant gradient tends to infinity. The regularized model then reads:*

$$\begin{cases} \partial_t n = \nabla_x (D_n \nabla_x n - n\, \chi(S)\, Q(\nabla_x S)) + H_1(n,S), \\ \partial_t S - D_S \Delta S = H_2(n,S), \end{cases} \tag{4.14}$$

where a smooth bounded chemotactic flux function $Q(x) = (Q_1(x), ..., D_d(x))$*, and* $x = (x_1, ..., x_d)^T$*, satisfies the following properties:*

$$Q(0) = 0, \quad |Q_i| \leq C_i, \quad \frac{\partial Q_i}{\partial x_i} > 0, \quad i = 1, ...d, \tag{4.15}$$

where C_i *are constants. This regularization is similar to the one proposed in [17] for the PKS system.*

The synthesized form of the saturated flux is a Pade approximate which connects universal features present at both very small and very large gradients. There is a certain arbitrariness in the choice of the chemotactic flux function Q*. A typical example of such function (see [17])*

$$Q(\nabla_x S) = \begin{cases} \nabla_x S, \quad if \quad |\nabla_x S| \leq x^\star, \\ \left(\dfrac{|\nabla_x S| - x^\star}{\sqrt{1 + |\nabla_x S - x^\star|^2}} + x^\star \right) \dfrac{\nabla_x S}{|\nabla_x S|}, \quad if \quad |\nabla_x S| > x^\star, \end{cases} \tag{4.16}$$

where $x^\star$ *is a switching parameter, which defines a small gradient values, for which the system (4.14) reduces to the original PKS system (2.28) so that the effect of saturated chemotactic flux function is felt at large gradient regimes only. Note that when* $x^\star = 0$*, the flux (4.16) becomes a mean curvature type function:*

$$Q(\nabla_x S) = \frac{\nabla_x S}{\sqrt{1 + |\nabla_x S|^2}}.$$

We investigate how the classical chemotaxis equations (4.14)-(4.15), which describe the population-level response to external chemical signals, can be obtained from the microscopic description delivered by model (3.1), as well as some more precise approaches to the several phenomena described in the previous items. If we combine the relaxation kernels presented in (4.1) with

$$T_1^1[f_2] = K_{\frac{f_2}{M_2}}(v, v^*) \cdot Q(\nabla_x (\frac{f_2}{M_2})), \tag{4.17}$$

where K satisfies (4.7), and Q satisfies (4.15), and moreover assumed to satisfy the following:

$$Q(x+\varepsilon y) = Q(x) + O(\varepsilon), \quad as \quad \varepsilon \to 0. \tag{4.18}$$

Then T_1^1 satisfies (2.24), and consequently, chemotaxis type models for optimal drift following the chemoattractant are obtained:

$$\begin{cases} \partial_t n + div_x \left(n\,\chi(S)\cdot Q(\nabla_x S) + \varepsilon^{p-1}(\Gamma(n,S) - D_n \cdot \nabla_x n)\right) \\ \qquad\qquad -H_1(n,S) + O(\varepsilon) = 0, \\ \partial_t S + \varepsilon^{q-1} div_x(\beta(n,S) - D_S \cdot \nabla_x S) - H_2(n,S) + O(\varepsilon) = 0. \end{cases} \tag{4.19}$$

Let $p = q = 1$, and $G_{11} = G_{21} = 0$, then $\Gamma(n,S) = \beta(n,S) = 0$, and then from (4.19), macro-scale models (4.14) up to ε are obtained.

5. A coupled chemotaxis-fluid model

5.1. A macro-scale model of chemotaxis-fluid

Aquatic bacteria like Bacillus subtilis are heavier than water yet they are able to swim up an oxygen gradient and concentrate in a layer below the water surface, which will undergo RayleighTaylor-type instabilities for sufficiently high concentrations. In the literature, a simplified chemotaxis-fluid system has been proposed as a model for bioconvection in modestly diluted cell suspensions. It couples a convective chemotaxis system for the oxygen-consuming and oxytactic bacteria with the incompressible Navier-Stokes equations subject to a gravitational force proportional to the relative surplus of the cell density compared to the water density. In Hill, Pedley [26], Dombrowski et al. [19], Chertock et al. [16] and Tuval et al. [39], several related coupled chemotaxisfluid model systems have been proposed to describe the collective behaviour of a suspension of oxytactic bacteria in an incompressible fluid under the assumptions that the contribution of bacteria to the bacteria-fluid suspension is sufficiently small (since the density of the bacteria suspension is approximately equal to the density of the fluid) and that more detailed cell-cell interactions (such as hydrodynamic interaction) are neglected. This collective behaviour is also known as bio-convection, and can be described by the following system:

$$\begin{cases} \partial_t n + u\cdot\nabla_x n = \delta\Delta n - \ div_x(n\chi(S)\cdot\nabla_x S), \\ \partial_t S + u\cdot\nabla_x S = \mu\Delta S - k(S)n, \\ \partial_t u + u\cdot\nabla_x u + \nabla_x p = \nu\Delta u - n\nabla_x\phi, \\ div_x u = 0. \end{cases} \tag{5.1}$$

Here, the unknowns are $n = n(t, x)$, $S = S(t, x)$, $u(t, x) : \mathbb{R}^+ \times \Omega \longrightarrow \mathbb{R}^d$ and $p = p(t, x) : \mathbb{R}^+ \times \Omega \longrightarrow \mathbb{R}$, denoting the cell density, chemical concentration, velocity field and pressure of the fluid, respectively. $\Omega \subset \mathbb{R}^d$ is a spatial domain where the cells and the fluid move and interact. Positive constants δ, μ and ν are the corresponding diffusion coefficients for the cells, chemical and fluid. $\chi(S)$ is the chemotactic sensitivity and $k(S)$ is the consumption rate of the chemical by the cells. $\phi = \phi(x)$ is a given potential function accounting the effects of external forces such as gravity.

It can be noticed from (5.1) that chemotaxis and fluid are coupled through both the transport of the cells and the chemical $u \cdot \nabla_x n$, $u \cdot \nabla_x S$ by the fluid and the external force $-n\nabla_x \phi$ exerted on the fluid by the cells.

5.2. A general approach toward micro-macro derivation of chemotaxis-fluid phenomena

This subsection presents a general approach to the derivation of macro-scale tissue models, where the movement of cells is induced by additional bio-chemical substances which are homogeneously distributed in space with a density that evolves in time due both to interactions and natural decay. This mathematical structure will be subsequently used to derive macro-scale models including those reviewed in Subsection 5.1. The contents is presented in three subsections, the first one proposes a two-scale model kinetic and continuous, the following one derives a general model for a variety of chemotaxis phenomena, while the last one shows how the approach leads, under appropriate assumptions, to the model (5.1).

5.2.1. A two-scale kinetic-continuous framework

Now consider the two scale kinetic-macro models given in the following:

$$\begin{cases} \big(\varepsilon \partial_t + v \cdot \nabla_x\big) f_1^\varepsilon = \frac{1}{\varepsilon^p} \mathcal{T}_1[f_2^\varepsilon](f_1^\varepsilon) + G_1(f_1, f_2, u, v), \\ \big(\varepsilon \partial_t + v \cdot \nabla_x\big) f_2^\varepsilon = \frac{1}{\varepsilon^q} \mathcal{T}_2(f_2^\varepsilon) + G_2(f_1, f_2, u, v), \\ \partial_t u + u \cdot \nabla_x u + \nabla_x p = \nu \Delta u - n \nabla_x \phi, \\ div_x u = 0, \end{cases} \tag{5.2}$$

where f_1, f_2 denote the density of cell, and chemical concentration, depending on time t, position $x \in \Omega \subset \mathbb{R}^d$ and velocity $v \in V \subset \mathbb{R}^d$. The functions $u(t, x)$, and $p(t, x)$ denote velocity field and pressure of the fluid, while G_1, G_2 are interactions terms that we suppose depending on the fluid velocity u, and assumed to satisfy the following:

$$G_i(f_1, f_2, u, v) = G_{i1}(f_1, f_2, u, v) + \varepsilon G_{i2}(f_1, f_2, v), \quad i = 1, 2, \tag{5.3}$$

where

$$\int_V G_{i1}(f_1, f_2, u, v) dv = 0, \quad i = 1, 2, \tag{5.4}$$

and G_{i1} are assumed to satisfy the following behavior as $\varepsilon \to 0$:

$$G_{ij}(M_1(v)n+\varepsilon g_1, M_2(v)S+\varepsilon g_2, u, v) = G_{ij}(M_1(v)n, M_2(v)S, u, v)+O(\varepsilon), \quad i, j = 1, 2. \tag{5.5}$$

The operators $\mathcal{T}_1, \mathcal{T}_2$ are still given by (2.2), and assumed to satisfy Assumptions (2.4)-(2.10).

5.2.2. Derivation of a general chemotaxis-fluid model

The results of Section 4 can be applied to (5.2) to deduce finally the macro-scale chemotaxis-fluid type models given by the following:

$$\begin{cases} \partial_t n + div_x\,(n\,\alpha(S) + \varepsilon^{p-1}(\Gamma(n, S, u) - D_n \cdot \nabla_x n)) - H_1(n, S) + O(\varepsilon) = 0, \\[2ex] \partial_t S + \varepsilon^{q-1} div_x(\beta(n, S, u) - D_S \cdot \nabla_x S) - H_2(n, S) + O(\varepsilon) = 0, \\[2ex] \partial_t u + u \cdot \nabla_x u + \nabla_x p = \nu \Delta u - n \nabla_x \phi, \\[2ex] div_x u = 0. \end{cases} \tag{5.6}$$

where $\alpha, \Gamma, \beta, D_n, D_s$, and H_1, H_2 are given respectively by (4.3)-(4.5) and H_1, H_2 are still given by (3.14).

The approach we have developed is quite general. A specific example (5.1) is reported in the following.

5.2.3. Example: Derivation of coupled chemotaxis-fluid model

As an example of the above analysis, we consider the case where the set for velocity is the sphere of radius $r > 0, V = rS^{d-1}$. Let (f_1, f_2, u) be a solution of (5.2), where we assume that the kernels $T_1^1[f_2]$ is given by (4.6), and $T_1^0(v, v') = \frac{\sigma_1}{|V|}$, $T_2(v, v') = \frac{\sigma_2}{|V|}$, $(\sigma_1, \sigma_2 > 0)$. Then the operators $\mathcal{T}_1^0(f)$, and $\mathcal{T}_2(f)$ are the relaxation operators:

$$\mathcal{T}_1^0(f) = \frac{\sigma_1}{\mid V \mid}\Big(\langle f \rangle - \mid V \mid f(v)\Big), \tag{5.7}$$

$$\mathcal{T}_2(f) = \frac{\sigma_2}{\mid V \mid}\Big(\langle f \rangle - \mid V \mid f(v)\Big). \tag{5.8}$$

In particular Assumptions 2.1 and 2.2 are satisfied, and the solutions $\theta_1(v)$, and $\theta_2(v)$ of $\mathcal{T}_1^0(\theta_1(v)) = vM_1(v)$, and $\mathcal{T}_2(\theta_2(v)) = vM_2(v)$ are given by

$$\theta_1(v) = -\frac{v}{\mid V \mid \sigma_1}, \quad \theta_2(v) = -\frac{v}{\mid V \mid \sigma_2}.$$

Therefore the diffusion tensors D_n and D_S are isotropic and are given by:

$$D_n = \frac{1}{\mid V \mid \sigma_1}\int_V v \otimes v dv = \frac{r^2}{\sigma_1 d} I, \quad D_S = \frac{1}{\mid V \mid \sigma_2}\int_V v \otimes v dv = \frac{r^2}{\sigma_2 d} I.$$

Let now

$$G_{11}(f_1, f_2, u, v) = \frac{d\sigma_1}{r^2 \mid V \mid}\langle f_1\rangle\, v \cdot u, \quad G_{21}(f_1, f_2, u, v) = \frac{\sigma_2 d}{r^2 \mid V \mid}\langle f_2\rangle\, v \cdot u. \tag{5.9}$$

It is plain that G_{11} and G_{21} satisfies (5.4)-(5.5), and then the terms Γ and β can be computed from (3.12)-(3.13) as follows:

$$\Gamma(n, S, u) = \frac{d}{r^2 \mid V \mid}\int_V v(v \cdot u) n dv = \frac{d}{r^2 \mid V \mid}(\int_V v \otimes v dv) \cdot (nu) = nu,$$

$$\beta(n, S, u) = \frac{d}{r^2 \mid V \mid}\int_V v(v \cdot u) S dv = \frac{d}{r^2 \mid V \mid}(\int_V v \otimes v dv) \cdot (Su) = Su.$$

Moreover, as $div_x u = 0$ then one has

$$div_x(\Gamma(n, S, u)) = u \cdot \nabla_x n, \quad div_x(\beta(n, S, u)) = u \cdot \nabla_x S. \tag{5.10}$$

In detail, let us consider in (5.2) the following:

$$G_{12} = 0, \quad G_{22}(f_1, f_2, v) = -k(\mid V \mid f_2) f_1.$$

Therefore

$$H_1(n, S) = 0, \quad H_2(n, S) = -\frac{1}{\mid V \mid}\int_V k(S) n dv = -k(S) n. \tag{5.11}$$

Finally, letting $p = q = 1$ in (5.6), using (5.10)-(5.11), one obtains the macroscopic coupled chemotax-is-fluid model model (5.1) up to ε:

$$\begin{cases} \partial_t n + u \cdot \nabla_x n = \delta \Delta n - \, div_x(n\chi(S) \cdot \nabla_x S) + O(\varepsilon), \\ \partial_t S + u \cdot \nabla_x S = \mu \Delta S - k(S) n, \, + O(\varepsilon), \\ \partial_t u + u \cdot \nabla_x u + \nabla_x p = \nu \Delta u - n \nabla_c \phi, \\ div_x u = 0, \end{cases} \tag{5.12}$$

where the corresponding diffusion coefficients for the cells, and chemical are given by:

$$\delta = \frac{r^2}{\sigma_1 d}, \quad \mu = \frac{r^2}{\sigma_2 d},$$

and the chemotaxis sensitivity χ is given by (4.8).

6. Perspectives

This paper presented a new approach to derive macro-scale models in biology from the underlying description at a cellular scale delivered by suitable developments of methods of kinetic theory and statistical mechanics. The hallmark that has guided the developments of the contents is that this micro-macro approach should replace the traditional one where conservation equations are closed by heuristic models of material behaviours, that generally hold true only in equilibrium conditions of for small deviations from equilibrium.

The application has been addressed mainly to a revisiting of the Keller and Segel model by showing how different modifications of the original model can be justified by a detailed analysis of interaction at the cellular scale. The new models appear to be more consistent with biological reality than the original one, which shows the not realistic feature of blow up of solutions. On the other hand, flux limited models appear to be more appropriated to biological tissues as it is properly studied in [40]. Moreover, nonlocal interactions are included as these are a typical feature of living systems [21].

The authors feel confident to state that this approach is general enough to be addressed to treat a variety of problems in life sciences for instance by the technically simple generalization to more than two interacting populations opens to a variety of interesting biological phenomena such as angiogenesis [1, 15] or tumor tissue evolution under the immune competition [11] related to Darwinian mutations at selection at the scale of cells.

Of course the main problem remains including in the micro-scale state also the biological functions expressed by cells and in referring them to the dynamics at the lower molecular scale (sub-cellular) this topic is far from having an exhaustive reply from the scientific community although some interesting results have recently appeared in the literature [13, 37]. The implication to the approach presented in this paper is very important as it gives the hint to study macro-scale models whose features evolve in time due to the dynamics at the molecular scale.

Acknowledgment

This work is supported by Hassan II Academy of Sciences and Technology (Morocco), Project 'Méthodes mathématiques et outils de modélisation et simulation pour le cancer'.

References

[1] *A.R.A. Anderson and V. Quaranta,* Integrative mathematical oncology, *Nature Reviews - Cancer,* **8***, (2008), 227–234.*

[2] N. Bellomo and A. Bellouquid, *From a class of kinetic models to the macroscopic equations for multicellular systems in biology,* Disc. Cont. Dyn. Syst. - Series B, **4**, *(2004), 59–80.*

[3] N. Bellomo, A. Bellouquid and M.A. Herrero, *From microscopic to macroscopic description of multicellular systems and biological growing tissues,* Comp. Math. Appl., **53**, *(2007), 647–663.*

[4] N. Bellomo, A. Bellouquid, J. Nieto, and J. Soler, *Multicellular growing systems: Hyperbolic limits towards macroscopic description,* Math. Mod. Meth. Appl. Sci., **17**, *(2007), 1675–1693.*

[5] N. Bellomo, A. Bellouquid, J. Nieto, and J. Soler, *Multiscale derivation of biological tissues models for mixtures of multicellular growing systems: application to flux–limited chemotaxis,* Math. Mod. Meth. Appl. Sci., **20**, *(2010), 1179–1207.*

[6] N. Bellomo, A. Bellouquid, J. Nieto, and J. Soler, *On the asymptotic theory from microscopic to macroscopic growing tissue models: an overview with perspectives,* Math. Mod. Meth. Appl. Sci., **22**, *(2012), 1130001 (37 pages).*

[7] N. Bellomo, A. Bellouquid, N. Nieto, and J. Soler, *Modeling chemotaxis from L^2 closure moments in kinetic theory of active particles,* Disc. Cont. Dyn. Syst. - Series B, **18**, *(2013), 847-863.*

[8] A. Bellouquid, *Commentary to the paper "Morphogenetic action through flux-limited spreading",* Phys Life Rev., **4**, *(2013), 477-478.*

[9] A. Bellouquid, *Mathematical tools towards the modelling of biological system: an overview and perspectives,* International Journal of Cancer Research and Diagnosis., **1**, *(2013), 1-3.*

[10] A. Bellouquid and E. De Angelis, *From Kinetic Models of Multicellular Growing Systems to Macroscopic Biological Tissue Models,* Nonlinear Analysis: Real World. Appl., **12**, *(2011), 1111–1122.*

[11] A. Bellouquid, E. De Angelis, and D. Knopoff, *From the modeling of the immune hallmarks of cancer to a black swan in biology,* Math. Mod. Meth. Appl. Sci., **23**, *(2013), 949–978.*

[12] F.A. Chalub, Y. Dolak-Struss, P. Markowich, D. Oeltz, C. Schmeiser C., and Soref A., Model hierarchies for cell aggregation by chemotaxis, *Math. Mod. Meth. Appl. Sci.,* **16***, (2006), 1173–1198.*

[13] J. Calvo, J. Nieto, J. Soler, and M.O. Vasquez, *On a dispersive model for unzipping of double-strained DNA molecules* Math. Mod. Meth. Appl. Sci., **24**, *(2014),* to appear.

[14] F.A. Chalub, P. Markovich, B. Perthame, and C. Schmeiser, *Kinetic models for chemotaxis and their drift–diffusion limits*, Monatsh. Math., **142**, *(2004), 123–141.*

[15] Chaplain M.A.J., Mathematical modeling of angiogenesis, J. of Neuro-Oncology, **50**, *(2000), 37–51.*

[16] A. Chertock, K. Fellner, A. Kurganov, A. Lorz, and P.A. Markowich, Sinking, merging and stationary plumes in a coupled chemotaxis-fuid model: a high-resolution numerical approach, J. Fluid Mech., **694**, *(2012), 155–190.*

[17] A. Chertock, A. Kurganov, X. Wang, and Y. Wu, On a chemotaxis model with saturated chemotactic flux, Kinetic Rel. Models, **5**, *(2012), 51–95.*

[18] Y. Dolak and T. Hillen, Cattaneo models for chemotaxis, numerical solution and pattern formation, J. Math. Biol., **2**, *(2003), 153–170.*

[19] C. Dombowski, L. Cisneros, S. Chatkaew, R. Goldstein, and J. Kesslerm Self-concentration and large-scale coherence in bacterial dynamics, Phys. Rev. Lett., **93**, *(2004), paper n.098103.*

[20] H. Du, Z. Xu, J.D. Shrout, and M. Alber, Multiscale modeling of Pesudomonas Aeruginosa swarming, Math. Mod. Meth. Appl. Sci., **21**, *(2011), 939–954.*

[21] R. Eftimie, Hyperbolic and kinetic models for self-organized biological aggregations and movement: a brief review, J. Math. Biol., **65**, *(2012), 35–75.*

[22] F. Filbet, P. Laurençot, and B. Perthame, Derivation of hyperbolic models for chemosensitive movement, J. Math. Biol., **50**, *(2005), 189–207.*

[23] J. Folkman, Role of angiogenesis in tumor growth and methastasis, Seminar Oncology, **29**, *(2002), 15–18.*

[24] M.A. Herrero, A. Köhn, and J.M. Pérez-Pomares, Modelling vascular morphogenesis: Current view on blood vessels development, Math. Mod. Meth. Appl. Sci., **19**, *(2009), 1483–1538.*

[25] T. Hillen and H.G. Othmer, The diffusion limit of transport equations derived from velocity jump processes, SIAM J. Appl. Math., **61(3)**, *(2000), 751–775.*

[26] N.A. Hill and T.J. Pedley, *Bioconvection*, Fluid Dyn. Res. **37**, *(2005), 1-20.*

[27] E.F. Keller, *Assessing the Keller–Segel model: how has it fared? In biological growth and spread*, Proc. Conf. Math. Biol. Heidelberg, Springer, Berlin, (1980), 379-387.

[28] E.F. Keller and L.A. Segel, Initiation od slide mold aggregation viewed as an instability, J. Theor. Biol., **26**, *(1970), 399–415.*

[29] E.F. Keller and L.A. Segel, Model for chemotaxis, J. Theor. Biol., **30**, *(1971), 225–234.*

[30] *E.F. Keller and L.A. Segel,* Traveling Bands of chemotactic Bacteria: A Theoretical Analysis, *J. Theor. Biol.,* **30**, *(1971), 235-248.*

[31] *P. Koumoutsakos, B. Bayati, F. Milde and G. Tauriello,* Particle simulations of morphogenesis, *Math. Mod. Meth. Appl. Sci.,* ***21***, *(2011), 955–1006.*

[32] *M. Lachowicz,* Micro and meso scales of description corresponding to a model of tissue invasion by solid tumors, *Math. Mod. Meth. Appl. Sci.,* **15**, *(2005), 1667–1683.*

[33] *M. Lemou and L. Mieussens,* A new asymptotic preserving scheme based on micromacro formulation for linear kinetic equations in the diffusion limit, *SIAM J. Sci. Comput.,* **31(1)**, *(2008), 334–368.*

[34] *M. Negreanu and J. Tello,* On a competitive system under chemotactic effects with non-local terms, *Nonlinearity* **26**, *(2013), 1083-1103.*

[35] *H.G. Othmer, S.R. Dunbar, and W. Alt,* Models of dispersal in biological systems, *J. Math. Biol.,* **26**, *(1988), 263–298.*

[36] *H.G. Othmer and T. Hillen,* The diffusion limit of transport equations II: chemotaxis equations, *SIAM J. Appl. Math.,* **62**, *(2002), 1222–1250.*

[37] *R. Rudnicki and J. Tiuryn, Size distribution of gene families in a genome, Math. Mod. Meth. Appl. Sci.,* **24**, *(2014), to appear.*

[38] *J. Tello and M. Winkler, A chemotaxis system with logistic source Commun. Partial Diff. Eqns,* **32**, *(2007), 49–87.*

[39] *I. Tuval, L. Cisneros, C. Dombrowski, C. Wolgemuth, J. Kessler, and R. Goldstein, Bacterial swimming and oxygen transport near contact lines, Proc. Natl. Acad. Sci.* **102**, *(2005), 2277-2282.*

[40] *M. Verbeni, O. Sanchez, E. Mollica, I. Siegl-Cachedenier, A. Carleton, I. Guerrero, A. Ruiz i Altaba, J. Soler,* Morphogenetic action through flux-limited spreading *Phys. Life Rev.,* **10**, *(2013), 457–475.*

The structure of some 2-groups and the capitulation problem for certain biquadratic fields

Abdelmalek Azizi[1] **and Mohammed Talbi**[2]

[1] ACSA Laboratory, Faculty of Sciences, University Mohamed Premier, Oujda, Morocco.
[2] Regional Center for Education and Training, Oujda, Morocco.
Corresponding Author E-mail: abdelmalekazizi@yahoo.fr

Abstract. *We study the capitulation problem for certain number fields K of degree 4 and we show how we can determine the structures of some 2-groups as an application of this study. Let $K_1^{(2)}$ be the Hilbert 2-class field of K, $K_2^{(2)}$ be the Hilbert 2-class field of $K_1^{(2)}$, $C_{K,2}$ be the 2-component of the ideal class group of K and G_2 the Galois group of $K_2^{(2)}/K$. We suppose that $C_{K,2}$ is of type $(2,2)$; then $K_1^{(2)}$ contains three extensions F_i/K, $i=1,2,3$. The aim of this paper is to study the capitulation of the 2-ideal classes in F_i, $i=1,2,3$, and as an application of this study, to determine the structure of G_2 and the structure of the 2-class group of the three fields F_i, $i=1,2,3$, for the following cases:*

(I) $K=\mathbb{Q}(\sqrt{2q_1q_2}, i)$ **where** q_1 **and** q_2 **are primes such that** $q_1\equiv q_2\equiv -1 \bmod 4$**. This is a case of biquadratic bicyclic number fields of** $\mathbb{Q}$**.**

(II) $K=\mathbb{Q}(\sqrt{-pq(2+\sqrt{2})})$ **where** p **and** q **are primes such that** $p\equiv -q\equiv 5 \bmod 8$**. This is a case of quartic number fields of** $\mathbb{Q}$**.**

Key words: unit, class group, capitulation, Hilbert class field.

1. Intoduction

Let K be a number field of finite degree over $\mathbb{Q}$ and C_K be the class group of K. Let F be an unramified extension of K of finite degree and let O_F be its ring of integers. We say that an ideal $\mathcal{A}$ (or the ideal class of $\mathcal{A}$) of K capitulates in F if it becomes principal in F, i.e., if $\mathcal{A}O_F$ is principal in F. The Hilbert class field K_1 of K is the maximal abelian unramified extension of K. Let p be a prime number; the Hilbert p-class field $K_1^{(p)}$ of K is the maximal abelian unramified extension of K such that $[K_1^{(p)} : K] = p^n$ for some integer n. The first important result on capitulation was conjectured by D. Hilbert and proved by E. Artin and P. Furtwängler. It deals with the case $F = K_1$.

Theorem 1 (Principal ideal theorem)**.** *Let K_1 be the Hilbert class field of K, then every ideal of K capitulates in K_1.*

The principal ideal theorem was generalized by Tannaka and Terada to the next one. Let K_0 be a subfield of K such that K/K_0 is abelian and let $(K/K_0)^*$ be the relative genus field of K/K_0.

Theorem 2 (Tannaka–Terada)**.** *If K/K_0 is cyclic, then any ambiguous ideal class of K/K_0 is principal in $(K/K_0)^*$.*

The case where F/K is a cyclic extension of prime degree was studied by D. Hilbert in his Theorem 94:

Theorem 3 (Theorem 94)**.** *Let F/K be a cyclic extension of prime degree, then there exists at least one class (not trivial) in K which capitulates in F.*

We find in the proof of Theorem 94 this result:
Let σ be a generator of the Galois group of F/K and $N_{F/K}$ be the norm of F/K. Let E_F be the unit group of the field F. Let E_F^* be the group of units of norm 1 in F/K. Then the group of classes of K which capitulates in F is isomorphic to the quotient group $E_F^*/E_F^{1-\sigma} = H^1(E_F)$, the cohomology group of $G = \langle\sigma\rangle$ acting on the group E_F.
With this result and other results on cohomology, we have:

Theorem 4 ([11])**.** *Let F/K be a cyclic unramified extension of prime degree, then the number of classes which capitulate in F/K is equal to*

$$[F : K][E_K : N_{F/K}(E_F)],$$

where E_K (resp. E_F) is the unit group of K (resp. F).

The case where F/K is an abelian extension was treated by H. Suzuki who has proved Miyake's conjecture: *In an abelian extension F/K the number of classes of K which capitulates in F is a multiple of* $[F : K]$.
Moreover, H. Suzuki has proved the next theorem which is a generalization of the principal ideal theorem, the Hilbert theorem 94 and Tannaka-Terada's principal ideal theorem:

Theorem 5. *Let K be a finite cyclic extension of an algebraic number field K_0 of finite degree, and let F be an unramified extension of K which is abelian over K_0. Then the number of the $G(K/K_0)$-invariant ideal classes of K which become principal in F is divisible by the degree $[F : K]$ of the extension F/K.*

Let p be a prime number and let $K_1^{(p)}$ (resp. $K_2^{(p)}$) be the Hilbert p-class field of K (resp. of $K_1^{(p)}$). If L is a subfield of K_1 and $\mathcal{A}$ is an ideal class of K whose order is equal to p^m for some integer m, then $\mathcal{A}$ capitulates in L if and only if $\mathcal{A}$ capitulates in $L \cap K_1^{(p)}$. So we study only the capitulation of classes whose orders are equal to p^m in the subfields of $K_1^{(p)}$, and since the capitulation problem is solved when $K_1^{(p)}/K$ is cyclic, we study only the cases where $K_1^{(p)}/K$ is not cyclic.
For more details see [18], [20], [1] and [21].

Definition 6. *Let F be a cyclic unramified extension of K, C_F be its class field and j the application of C_K in C_F that maps to the class of an ideal $\mathfrak{a}$ of K, the class of the ideal generated by $\mathfrak{a}$ in F. Then the extension F/K is called:*

- *of type (A) if and only if $\# \ker j \cap N_{F/K}(C_F) > 1$;*
- *of type (B) if and only if $\# \ker j \cap N_{F/K}(C_F) = 1$.*

Proposition 7 ([14]). *Let G be a 2-group of finite order 2^m and G' its derived subgroup. Then G/G' is of type $(2,2)$ if and only if G is isomorphic to one of 2-groups:*

$$\begin{array}{llllll}
Q_m & = & <\sigma,\tau> & o & \sigma^{2^{m-2}} = \tau^2 = a, & a^2 = 1,\ \tau^{-1}\sigma\tau = \sigma^{-1}; \\
D_m & = & <\sigma,\tau> & o & \sigma^{2^{m-1}} = \tau^2 = 1, & \tau^{-1}\sigma\tau = \sigma^{-1}; \\
S_m & = & <\sigma,\tau> & o & \sigma^{2^{m-1}} = \tau^2 = 1, & \tau^{-1}\sigma\tau = \sigma^{2^{m-2}-1}; \\
(2,2) & = & <\sigma,\tau> & o & \sigma^2 = \tau^2 = 1, & \tau^{-1}\sigma\tau = \sigma.
\end{array}$$

Where Q_m the quaternion group, D_m the dihedral group, S_m semi-dihedral group of order 2^m and (2.2) is an abelian group isomorphic to $\mathbb{Z}/2\mathbb{Z} \times \mathbb{Z}/2\mathbb{Z}$.

Let K be a number field such that the 2-component $C_{K,2}$ of C_K is isomorphic to $\mathbb{Z}/2\mathbb{Z} \times \mathbb{Z}/2\mathbb{Z}$. Let G_2 be the Galois group of $K_2^{(2)}/K$. By class field theory, $Gal(K_1^{(2)}/K) \simeq \mathbb{Z}/2\mathbb{Z} \times \mathbb{Z}/2\mathbb{Z}$. Then $K_1^{(2)}$ contains three quadratic extensions of K denoted by F_1, F_2 and F_3; precisely F_1 is the subfield of $K_2^{(2)}$ left fixed by the subgroup $< \sigma >$, F_2 is the subfield of $K_2^{(2)}$ left fixed by the subgroup $< \sigma^2, \tau >$ and F_3 is the subfield of $K_2^{(2)}$ left fixed by the subgroup $< \sigma^2, \sigma\tau >$. Furthermore, if $G'_2 \neq 1$, then $K_1^{(2)} \neq K_2^{(2)}$ and there exists a unique subgroup of G'_2 of index 2; let L be the subfield of $K_2^{(2)}$ left fixed by this subgroup and j_i the mapping j defined for $F = F_i$. Under these conditions, H. Kisilevsky, in [14], proved the following

Theorem 8 ([14]). *Assume that $C_{K,2} \simeq \mathbb{Z}/2\mathbb{Z} \times \mathbb{Z}/2\mathbb{Z}$, so we have*

1. *If $K_2^{(1)} = K_2^{(2)}$, then the fields F_i are of type (A), $\# \ker j_i = 4$ for $i = 1, 2, 3$ and $G_2 \simeq \mathbb{Z}/2\mathbb{Z} \times \mathbb{Z}/2\mathbb{Z}$;*
2. *If $Gal(L/K) \simeq Q_3$, then the fields F_i are of type (A), $\# \ker j_i = 2$ for $i = 1, 2, 3$ and $G_2 \simeq Q_3$;*

3. *If $Gal(L/K) \simeq D_3$, then the fields F_2 and F_3 are of type (B) and $\# \ker j_2 = \# \ker j_3 = 2$. Moreover, if F_1 is of type (B) then $\# \ker j_1 = 2$ and $G_2 \simeq S_m$. If F_1 is of type (A) and $\# \ker j_1 = 2$, then $G_2 \simeq Q_m$. Finally if F_1 is of type (A) and $\# \ker j_1 = 4$, then $G_2 \simeq D_m$.*

Corollary 9. *Let K be such that $C_{K,2} \simeq \mathbb{Z}/2\mathbb{Z} \times \mathbb{Z}/2\mathbb{Z}$. Then we have three types of capitulation:*

Type 1*: The four classes of $C_{K,2}$ capitulate in each extension F_i, $i = 1, 2, 3$.*
This is possible if and only if $K_1^{(2)} = K_2^{(2)}$.
Type 2*: The four classes of $C_{K,2}$ capitulate only in one extension among the*
three extensions F_i, $i = 1, 2, 3$. In this case the group G_2 is dihedral.
Type 3*: Only two classes capitulate in each extension F_i, $i = 1,\ 2,\ 3$. In this*
case the group G_2 is semi-dihedral or quaternionic.

Remark 10. *The 2-class group of F_1 is cyclic. The 2-class groups of F_2 and F_3 are cyclic in the cases 1 and 2 of the theorem 8 and are of type $(2,2)$ in the third case.*

2. Units of some number fields

Let $d_1,\ d_2$ be coprime integers, which are square-free, $d_3 = d_1d_2$, ε_1 (resp. $\varepsilon_2, \varepsilon_3$) the fundamental unit of $\mathbb{Q}(\sqrt{d_1})$ (resp. $\mathbb{Q}(\sqrt{d_2})$, $\mathbb{Q}(\sqrt{d_3})$), $K_0 = \mathbb{Q}(\sqrt{d_1}, \sqrt{d_2})$, Q_{K_0} the Hasse unit index of K_0 and N_i the norm of $K_0/\mathbb{Q}(\sqrt{d_i})$ with $i \in \{1, 2, 3\}$.
From [15], we know that a fundamental system of units of K_0 is one of the following:

(i)	$\{\varepsilon_1, \varepsilon_2, \varepsilon_3\}$;	
(ii)	$\{\varepsilon_1, \varepsilon_2, \sqrt{\varepsilon_3}\}$	$(N_2(\varepsilon_3) = 1)$;
(iii)	$\{\sqrt{\varepsilon_1\varepsilon_2}, \varepsilon_2, \varepsilon_3\}$	$(N_3(\varepsilon_1) = N_3(\varepsilon_2) = 1)$;
(iv)	$\{\varepsilon_1, \sqrt{\varepsilon_2}, \sqrt{\varepsilon_3}\}$	$(N_1(\varepsilon_2) = N_1(\varepsilon_3) = 1)$;
(v)	$\{\sqrt{\varepsilon_1\varepsilon_2}, \sqrt{\varepsilon_2\varepsilon_3}, \sqrt{\varepsilon_1\varepsilon_3}\}$	$(N_2(\varepsilon_3) = N_3(\varepsilon_j) = 1, j = 1, 2)$;
(vi)	$\{\sqrt{\varepsilon_1\varepsilon_2\varepsilon_3}, \varepsilon_2, \varepsilon_3\}$	$(N_3(\varepsilon_1) = N_3(\varepsilon_2) = N_2(\varepsilon_3) = \pm 1)$.

Proposition 11 ([2])**.** *Let K_0 a real number field, $F = K_0(\sqrt{-1})$ a quadratic extension of K_0, abelian and finite over $\mathbb{Q}$ and $\{\varepsilon_1, \varepsilon_2, ..., \varepsilon_r\}$ be a fundamental system of units of K_0 $($whose units are all positive$)$. Then we have:*

1. *If there is a unit of K_0 of the form $\varepsilon = \varepsilon_1^{j_1}\varepsilon_2^{j_2}...\varepsilon_{r-1}^{j_{r-1}}\varepsilon_r$ where $j_k \in \{0, 1\}$, such that $(2 + \mu_m)\varepsilon$ is a square in K_0, then $\{\varepsilon_1, \varepsilon_2, ..., \varepsilon_{r-1}, \sqrt{\zeta_m\varepsilon}\}$ is a fundamental system of units of F;*
2. *Otherwise $\{\varepsilon_1, \varepsilon_2, ..., \varepsilon_r\}$ is a fundamental system of units of F.*

Proposition 12 ([2])**.** *Let K_0 a number field, abelian real and β an algebraic integer in K_0, completely positive, without square factors. Assume that $F = K_0(\sqrt{-\beta})$ is a quadratic extension of K_0, abelian over $\mathbb{Q}$ and $i = \sqrt{-1}$ doesn't belong to F. Let $\{\varepsilon_1, \varepsilon_2, ..., \varepsilon_r\}$ be a fundamental system of units of K_0. We choose, without limiting the generality, units ε_j positive. Then we have:*

1. *If there is a unit of K_0 such that $\varepsilon = \varepsilon_1^{j_1}\varepsilon_2^{j_2}...\varepsilon_{r-1}^{j_{r-1}}\varepsilon_r$ (close to a permutation), where the $j_k \in \{0, 1\}$, such that $\beta\varepsilon$ is a square in K_0, then $\{\varepsilon_1, \varepsilon_2, ..., \varepsilon_{r-1}, \sqrt{-\varepsilon}\}$ is a fundamental system of units of F;*

2. *Otherwise* $\{\varepsilon_1, \varepsilon_2, ..., \varepsilon_r\}$ *is a fundamental system of units of* F.

Corollary 13 ([7])**.** *Let* $L = \mathbb{Q}(\sqrt{-n\varepsilon\sqrt{d}})$ *be a cyclic extension of degree* 4 *over* $\mathbb{Q}$*, where* ε *is the fundamental unit of* $\mathbb{Q}(\sqrt{d})$ *with* d *a square-free integer and* n *an integer, then* $\{\varepsilon\}$ *is a fundamental system of units of* L.

Lemma 14 ([3], Theorem 14)**.** *Let* p *and* q *be odd prime numbers such as* $q \equiv -1 \bmod 4$, $K_0 = \mathbb{Q}(\sqrt{2}, \sqrt{pq})$, $F = K_0(i)$ *and* ε_1 (*resp.* ε_2, ε_3) *be the fundamental unit of* $\mathbb{Q}(\sqrt{2})$ (*resp.* $\mathbb{Q}(\sqrt{pq})$, $\mathbb{Q}(\sqrt{2pq})$. *Assume that* $2\varepsilon_3$ *is not a square in* $\mathbb{Q}(\sqrt{2pq})$ *and* $\varepsilon_2 = x + y\sqrt{pq}$ *with* $(x, y) \in \mathbb{Z}^2$. *Then we have:*

(i) *If* $x \pm 1$ *is a square in* $\mathbb{N}$*, then* $\{\varepsilon_1, \sqrt{\varepsilon_2}, \varepsilon_3\}$ *is a fundamental system of units of* K_0 *and of* F.

(ii) *Otherwise,* $\{\varepsilon_1, \varepsilon_2, \sqrt{\varepsilon_2\varepsilon_3}\}$ *is a fundamental system of units of* K_0 *and of* F.

Lemma 15 ([3], Theorem 14)**.** *We keep the notations of the previous lemma and assume that* p *and* q *are congruent to* -1 *modulo* 4*, and that* $2\varepsilon_3$ *is not a square in* $\mathbb{Q}(\sqrt{2pq})$ *and* $\varepsilon_2 = \frac{x}{2} + \frac{y}{2}\sqrt{pq}$ *with* x *and* y *be two odd integers. Then* K_0 *and* F *have the same fundamental system of units.*

Lemma 16. *Let* p, q *be odd prime numbers,* $K_0 = \mathbb{Q}(\sqrt{q}, \sqrt{2p})$, ε_1 (*resp.* ε_2, ε_3) *the fundamental unit of* $\mathbb{Q}(\sqrt{q})$ (*resp.* $\mathbb{Q}(\sqrt{2p})$, $\mathbb{Q}(\sqrt{2pq})$). *Assume that all units* ε_i *are of norm* 1 *and* $2\varepsilon_3$ *is not a square in* $\mathbb{Q}(\sqrt{2pq})$. *We set* $\varepsilon_3 = x + y\sqrt{2pq}$. *Then a fundamental system of units of* K_0 *is*

(i) $\{\sqrt{\varepsilon_1\varepsilon_3}, \sqrt{\varepsilon_1\varepsilon_2}, \sqrt{\varepsilon_2\varepsilon_3}\}$ *if* $2p(x \pm 1)$ *is a square in* $\mathbb{N}$.

(ii) $\{\varepsilon_1, \sqrt{\varepsilon_1\varepsilon_2}, \sqrt{\varepsilon_3}\}$ *if* $2q(x \pm 1)$ *is a square in* $\mathbb{N}$.

Proof. Let $\varepsilon_3 = x + y\sqrt{2pq}$ such that $(x-1)(x+1) = 2pqy^2$. We know that $2\varepsilon_3$ is a square in $\mathbb{Q}(\sqrt{2pq})$ if and only if $x \pm 1$ is a square in $\mathbb{N}$.
- If $2(x \pm 1)$ is a square in $\mathbb{N}$, then there exists $(y_1, y_2) \in \mathbb{Z}^2$ such that
$$\begin{cases} x \pm 1 = 2y_1^2 \\ x \mp 1 = pqy_2^2 \end{cases} \text{ and } \sqrt{\varepsilon_3} = \tfrac{1}{2}(y_2\sqrt{2pq} + 2y_1) \in \mathbb{Q}(\sqrt{2pq}).$$
This is contrary to the fact that ε_3 is the fundamental unit of $\mathbb{Q}(\sqrt{2pq})$. Following $2p(x \pm 1)$ or $2q(x \pm 1)$ is a square in $\mathbb{N}$.
- If $2p(x \pm 1)$ is a square in $\mathbb{N}$, then $q(x \mp 1)$ is a square in $\mathbb{N}$ and there exists $(y_1, y_2) \in \mathbb{Z}^2$ such that
$$\begin{cases} x \pm 1 = 2py_1^2 \\ x \mp 1 = qy_2^2 \end{cases} \text{ and } \begin{cases} \sqrt{2\varepsilon_3} = y_1\sqrt{2p} + y_2\sqrt{q} \\ \sqrt{\varepsilon_3} = \tfrac{1}{2}(2y_1\sqrt{p} + y_2\sqrt{2q}) \end{cases}.$$
- If $2q(x \pm 1)$ is a square in $\mathbb{N}$, then $p(x \mp 1)$ is a square in $\mathbb{N}$ and there exists $(y_1, y_2) \in \mathbb{Z}^2$ such that
$$\begin{cases} x \pm 1 = 2qy_1^2 \\ x \mp 1 = py_2^2 \end{cases} \text{ and } \begin{cases} \sqrt{2\varepsilon_3} = y_1\sqrt{2q} + y_2\sqrt{p} \\ \sqrt{\varepsilon_3} = \tfrac{1}{2}(2y_1\sqrt{q} + y_2\sqrt{2p}) \end{cases}.$$
Therefore, if $2p(x \pm 1)$ is a square in $\mathbb{N}$, then $2\varepsilon_3$ is a square in K_0 and if $2q(x \pm 1)$ is a square in $\mathbb{N}$, then ε_3 is a square in K_0. On the other hand, after the two previous lemmas, $2\varepsilon_1$ and $2\varepsilon_2$ are squares in K_0. Hence $\varepsilon_1\varepsilon_2$ is a square in K_0. Similarly, if $2\varepsilon_3$ is a square in K_0, then $\varepsilon_1\varepsilon_3$ and $\varepsilon_2\varepsilon_3$ are squares in K_0 and thus is a fundamental system of units of K_0. In the case where ε_3 is a square in K_0, the unit $\varepsilon_1\varepsilon_2\varepsilon_3$ is a square in K_0 and according to the results of [15] recalled the beginning of this paragraph, $\{\varepsilon_1, \sqrt{\varepsilon_1\varepsilon_2}, \sqrt{\varepsilon_3}\}$ is a fundamental system of units of K_0.

Lemma 17. *With the conditions of Lemma 16. Let $F = K_0(i)$, then*

(i) *if $2p(x \pm 1)$ is a square in $\mathbb{N}$, then $\{\sqrt{\varepsilon_1\varepsilon_2}, \sqrt{\varepsilon_1\varepsilon_3}, \sqrt{i\varepsilon_1\varepsilon_2\varepsilon_3}\}$ is a fundamental system of units of F;*

(ii) *if $2q(x \pm 1)$ is a square in $\mathbb{N}$, then $\{\sqrt{\varepsilon_1\varepsilon_2}, \sqrt{\varepsilon_3}, \sqrt{i\varepsilon_2}\}$ is a fundamental system of units of F.*

Proof. (i) Let $\varepsilon = \sqrt{\varepsilon_1\varepsilon_2}\sqrt{\varepsilon_1\varepsilon_3}\sqrt{\varepsilon_2\varepsilon_3} = \varepsilon_1(\sqrt{\varepsilon_2\varepsilon_3})^2$. We know from Proposition 11 that $\sqrt{i\varepsilon} \in F$ if and only if $\sqrt{2\varepsilon} \in K_0$. Since $2\varepsilon_1$ is a square in K_0, then 2ε is a square in K_0. A fundamental system of units of K_0 is given by the preceding lemma. Hence, by Proposition 11, $\{\sqrt{\varepsilon_1\varepsilon_2}, \sqrt{\varepsilon_1\varepsilon_3}, \sqrt{i\varepsilon_1\varepsilon_2\varepsilon_3}\}$ is a fundamental system of units of F.
(ii) Let $\varepsilon = \varepsilon_2$. We know from Lemma 16 that $2\varepsilon_2$ is a square in K_0 and Lemma 17 gives us a fundamental system of units of K_0. So while using Proposition 11, we find that $\{\sqrt{\varepsilon_1\varepsilon_2}, \sqrt{\varepsilon_3}, \sqrt{i\varepsilon_2}\}$ is a fundamental system of units of F.

Theorem 18 ([6])**.** *Let $K_0 = \mathbb{Q}(\sqrt{2}, \sqrt{p})$, ε_0 (resp. ε_2, ε_3) the fundamental unit of $\mathbb{Q}(\sqrt{2})$ (resp. $\mathbb{Q}(\sqrt{p})$, $\mathbb{Q}(\sqrt{2p})$) and $F = K_0(\sqrt{-m\varepsilon_0\sqrt{2}})$ where m is an odd integer. Then,*

1) *if ε_3 has norm 1, then $\{\varepsilon_0, \varepsilon_2, \sqrt{\varepsilon_3}\}$ is a fundamental system of units of K_0 and of F;*

2) *otherwise, $\{\sqrt{\varepsilon_0\varepsilon_2\varepsilon_3}, \varepsilon_2, \varepsilon_3\}$ is a fundamental system of units of K_0 and of F.*

Theorem 19. *Let $L = \mathbb{Q}(\sqrt{2 + \sqrt{2}})$ and $F = L(\sqrt{-m})$ where m is an odd integer and square-free. Then $\{\xi_3, \xi_5, \xi_7\}$ is a fundamental system of units of L and of F where $\xi_3 = 1 + \sqrt{2 + \sqrt{2}}$, $\xi_5 = 1 + \sqrt{2} + \sqrt{2 + \sqrt{2}}$ and $\xi_7 = 1 + \sqrt{2} + \sqrt{2}\sqrt{2 + \sqrt{2}}$.*

Proof. It is known in the literature that $\{\xi_3, \xi_5, \xi_7\}$ is a fundamental system of units of L (see eg [24], p. 144-145). Since $m\xi$ is not a square in L, for $\xi = {\xi'_1}^{j_1}{\xi'_2}^{j_2}\xi'_3$ where $\{\xi'_1, \xi'_2, \xi'_3\} = \{\xi_3, \xi_5, \xi_7\}$ and $j_1, j_2 \in \{0, 1\}$, then, according to the proposition 12, we find that the system $\{\xi_3, \xi_5, \xi_7\}$ is a fundamental system of units of F.

3. Case where K is a biquadratic bicyclic number field of $\mathbb{Q}$

Let Q be the Hasse unit index of K and let $C_{K,2}$ be the 2-component of the class group of K. Let $K^{(*)}$ be the genus field of K. In this section, we suppose that $K = \mathbb{Q}(\sqrt{2q_1q_2}, i)$ where $q_1 \equiv q_2 \equiv -1 \bmod 4$, $\left(\frac{q_1}{q_2}\right) = -\left(\frac{q_2}{q_1}\right) = 1$, $\left(\frac{2}{q_1}\right) = -\left(\frac{2}{q_2}\right) = 1$ and $Q = 1$, in which case, the group $C_{K,2}$ is of type $(2, 2)$ and $K^{(*)} = K_1^{(2)} = \mathbb{Q}(\sqrt{q_1}, \sqrt{q_2}, \sqrt{2}, i)$. So $K_1^{(2)}$ contains three extensions F'_i/K, $i = 1, 2, 3$. The aim of this section is to study the capitulation of the 2-ideal classes in F'_i, $i = 1, 2, 3$, and to determine the structure of G_2. So we have:
$F'_1 = K(\sqrt{q_1}) = \mathbb{Q}(\sqrt{q_1}, \sqrt{2q_2}, i)$, $F'_2 = K(\sqrt{q_2}) = \mathbb{Q}(\sqrt{q_2}, \sqrt{2q_1}, i)$ and $F'_3 = K(\sqrt{2}) = \mathbb{Q}(\sqrt{2}, \sqrt{q_1q_2}, i)$.

Theorem 20. *Let* $K = \mathbb{Q}(\sqrt{2q_1q_2}, i)$ *with* $(\frac{q_1}{q_2}) = -(\frac{q_2}{q_1}) = (\frac{2}{q_1}) = -(\frac{2}{q_2}) = 1$ *and the unit's index* Q *of* $\mathbb{Q}(\sqrt{2q_1q_2})$ *in* K *is equal to* 1. *Then only two classes of* K *capitulate in each extension* F'_i, $i = 1, 2, 3$ *and the group* G_2 *is semi-dihedral or quaternionic.*

Proof. To prove this theorem we will use the fact that in an unramified extension F/K of degree 2 the number of classes that capitulated in F is equal to $2[E_K : N_{F/K}(E_F)]$. Let ε_3 be the fundamental unit of $\mathbb{Q}(\sqrt{2q_1q_2})$, then E_K, the unit group of K, is generated by ε_3 and the complex number i; so we must compute $N_{F/K}(E_F)$ in each case of F($F = F'_i$, $i = 1, 2, 3$).
On the other hand, let $\varepsilon_2 = x + y\sqrt{q_1q_2}$ be the fundamental unit of $\mathbb{Q}(\sqrt{q_1q_2})$. Then

a) If x and y are integers, then exactly two classes of $C_{K,2}$ capitulate in F'_1. It is the same for F'_2, while in F'_3 the 4 classes capitulate if and only if $x \pm 1$ is a square in $\mathbb{N}$ (a fundamental system of F'_1 or F'_2 is given by lemma 2.3 and lemma 2.4 and for F'_3 is given by lemma 2.1 and lemma 2.2). Let us show that $x \pm 1$ is never a square of $\mathbb{N}$.
Since $q_1q_2 \equiv 1 \bmod 4$, then x is odd. Therefore, the greatest common divisor of $x - 1$ and $x + 1$ is equal to two. Moreover, using the equation $(x - 1)(x + 1) = q_1q_2y^2$, we deduce that the exponent of 2 in the decomposition of $x - 1$ and $x + 1$ into prime factors is odd. It follows that $x \pm 1$ can not be a square in $\mathbb{N}$. Thus, our result is proved.

b) If x and y are half-integers. Then in each extension F'_i, ($i \in \{1, 2, 3\}$), exactly two classes of K capitulate. Indeed, in this case a fundamental system of units of K_3 and F'_3 is $\{\varepsilon_1, \varepsilon_2, \sqrt{\varepsilon_2\varepsilon_3}\}$. Then we have that $N(E_{F_3}) = E_K$. As a result, there are two classes that capitulated in F'_3. It is the same for the extensions F'_1 and F'_2.

Then only two classes of K capitulate in each extension F'_i, $i = 1, 2, 3$. Therefore, by theorem 8 and corollary 9, G_2 is the quaternionic group or semi-dihedral group.

Theorem 21. *Let* $K = \mathbb{Q}(\sqrt{2q_1q_2}, i)$ *with* $(\frac{q_1}{q_2}) = -(\frac{q_2}{q_1}) = (\frac{2}{q_1}) = -(\frac{2}{q_2}) = 1$ *and the unit index* Q *of* $\mathbb{Q}(\sqrt{2q_1q_2})$ *in* K *is equal to* 1. *Let* $F'_1 = K(\sqrt{q_1})$, $F'_2 = K(\sqrt{q_2})$ *and* $F'_3 = K(\sqrt{2})$, *then the* 2*-class groups of* F'_1 *and* F'_3 *are of type* $(2, 2)$ *and the* 2*-class groups of* F'_2 *is cyclic.*

Proof. Using Wada's formula on class number of multiquadratic fields ([23]) and Kaplan's results on the 2-part of class number of quadratic fields ([13]); then we have:
- $h(q_1)$, $h(q_2)$, $h(2q_1)$, $h(2q_2)$, $h(-q_1)$, $h(-q_2)$ et $h(q_1q_2)$ are odd;
- the 2-part of $h(-2q_2)$ is equal to 2, the 2-part of $h(-2q_1)$ is divided by 4 and is divided by 8 if and only if $q_1 \equiv 15 \bmod 16$, and the 2-part of $h(-q_1q_2)$ is equal to 4;
- let Q' be the index of the product of the units groups of all the quadratic fields which are subsets of F in the unit group of F (if $F = F'_i$; then $Q' = [E_{F'_i} : E_{-1}E_{q_1}E_{-q_1}E_{2q_2}E_{-2q_2}E_{2q_1q_2}E_{-2q_1q_2}]$).

Then we have

$$\begin{aligned}h(F_1') &= \frac{1}{2^5}Q'h(q_1)h(2q_2)h(-q_1)h(-2q_2)h(2q_1q_2)h(-2q_1q_2),\\ h(F_2') &= \frac{1}{2^5}Q'h(q_2)h(2q_1)h(-q_2)h(-2q_1)h(2q_2q_1)h(-2q_1q_2),\\ h(F_3') &= \frac{1}{2^5}Q'h(q_1q_2)h(2q_2)h(-q_1q_2)h(2q_1q_2)h(-2q_1q_2),\\ h(K) &= \frac{1}{2}h(2q_1q_2)h(-2q_1q_2).\end{aligned}$$

-$h(-2q_1q_2)h(2q_1q_2) = 8$ since the 2-class number of K is equal to 4.
- $Q' = 8$ for F_1' and F_2' and for F_3' we have $Q' = 4$; so the 2-class numbers of F_1' and F_3' are equal to 4 and the 2-class number of F_2' is divided by 8 and is divided by 16 if and only if $q_1 \equiv 15 \bmod 16$. Then we conclude that the order of G_2 is at least equal to 2^4 and that the 2-class number of F_1' and F_3' is equal to 4 and the 2-class number of F_2' is divided by 8. Then, by theorem 8 and with the use of the definition of F_i', $i = 1, 2, 3$ as fixed fields of sub-groups of index 2 of G_2, the 2-class groups of F_1' and F_3' are of type $(2, 2)$ and the 2-class groups of F_2' is cyclic.

Corollary 22. *Let* $K = \mathbb{Q}(\sqrt{2q_1q_2}, i)$ *with* $(\frac{q_1}{q_2}) = -(\frac{q_2}{q_1}) = (\frac{2}{q_1}) = -(\frac{2}{q_2}) = 1$ *and the unit index* Q *of* $\mathbb{Q}(\sqrt{2q_1q_2})$ *in* K *is equal to* 1. *Then the group* G_2 *is semi-dihedral.*

Proof. The 2-class group of K can be generated by classes of prime ideals of K laying above the ramified primes in $K/\mathbb{Q}$. But in our case this is not possible, we have only one non trivial class generated by the prime ideal I_0 above the prime 2 ($2O_K = I_0^4$). We choose the second generator as the following:
Let l be a prime such that $(\frac{q_1}{l}) = (\frac{q_2}{l}) = -1$ and $(\frac{2}{l}) = (\frac{-1}{l}) = 1$. The prime l exists (see [Sim-95]) and splits completely in $K/\mathbb{Q}$, then there exist some ideals I_1, I_2, I_3 and I_4 of K such that $lO_K = I_1I_2I_3I_4$. The ideal I_1 is inert in F_2'/K, so by the Artin Reciprocity theorem we prove that I_1 is not principal and, if m is the odd part of the class number of K, I_1^m is also not principal. Then $C_{K,2}$ is generated by the class of I_0 and the class of I_1^m.
The ideal I_1 is inert in F_2'/K. Also the ideal I_0 is inert in F_2'/K. So we have
- the ideal class of I_1^m isn't norm in F_2'/K.
- the ideal class of I_0 isn't norm in F_2'/K.
- the ideal class of $I_0I_1^m$ isn't norm in F_2'/K.
From these remarks and with using theorem 8, we obtain that one class from the classes of I_0, I_1^m or $I_0I_1^m$ capitulates in F_2'/K and it isn't norm from F_2'; so F_2' is of type (B). The field F_2' of our case is the field F_1 in theorem 8, so by this theorem the group G_2 is semi-dihedral.

Example 23. *Let* $q_1 = 7, q_2 = 3$ *and* $d = 2q_1q_2 = 42$.
The 2-*class group of of* $K = \mathbb{Q}(\sqrt{42}, i)$ *is of type* $(2, 2)$, $F_1' = K(\sqrt{7})$, $F_2' = K(\sqrt{3})$ *and* $F_3' = K(\sqrt{2})$. *Then only two classes of* K *capitulates in each extension* F_i', $i = 1, 2, 3$. *Moreover, in this case, the* 2-*class group of* F_2' *is cyclic of order* 8 *and* G_2 *is semi-dihedral of order* 16.

4. Case where K is a quartic number field of $\mathbb{Q}$

In this section, we suppose that $K = \mathbb{Q}(\sqrt{-pq(2+\sqrt{2})})$ where p and q are primes such that $p \equiv -q \equiv 5 \bmod 8$, in which case, the group $C_{K,2}$ is of type $(2,2)$ (see [8]), by using the results of [12] we show that the genus field of K is $K^{(*)} = K_1^{(2)} = K(\sqrt{p}, \sqrt{-q})$. So $K_1^{(2)}$ contains three extensions F_i'/K, $i = 1,2,3$. The aim of this section is to study the capitulation of the 2-ideal classes in F_i', $i = 1,2,3$, and to determine the structure of G_2. So we have: $F_1' = K(\sqrt{p})$, $F_2' = K(\sqrt{-q})$ and $F_3' = K(\sqrt{-pq})$.

Proposition 24. *Let L/M be a CM-extension, Δ its Galois group, and v_0 a place of M such that the following conditions hold:*

1) $C_{M,2} = 0$*;*

2) *L and M have the same units (hence $\sqrt{-1} \notin L$);*

3) *$L = M(\sqrt{\beta})$ with $\beta \in M$, and $2 \nmid v_0(\beta)$.*

then the natural map

$$\bigoplus_{\substack{v \in Ram(L/M) \\ v \neq v_0}} \mathbb{Z}/2\mathbb{Z} \rightarrow C_{L,2}$$

which, to a ramified place of M associates the class of its square root in L, is injective.

Proof. Let $I_{2,L}$ (resp. $I_{2,M}$) the group of fractional ideals of L tensored with $\mathbb{Z}_2$ (resp. M), and $P_{2,L}$ (resp. $P_{2,M}$) its sub $\mathbb{Z}_2$-module generated by the principal ideals. Let us analyze the image of the natural map $(I_{2,L})^{\Delta} \rightarrow (C_{L,2})^{\Delta}$. Thanks to (1), it factors into a map

$$\phi : (I_{2,L})^{\Delta}/I_{2,M} \rightarrow (C_{L,2})^{\Delta}$$

(here we embed $I_{2,M}$ into $I_{2,L}$ via the obvious map) which kernel is

$$(P_{2,L})^{\Delta}/I_{2,M} = (P_{2,L})^{\Delta}/P_{2,M} \simeq \operatorname{coker}((L^{\times})^{\Delta} \rightarrow (P_{2,L})^{\Delta}) \simeq H^1(\Delta, \mathcal{O}_L^{\times}).$$

Thanks to (2), we conclude that $\ker\phi$ is of order 2. Now, because of (3), $(\sqrt{\beta})$ gives a non trivial element of $\ker\phi$, hence generates it. The claimed result followed by explicitly writing ϕ as

$$\phi : \bigoplus_{v \in Ram(L/M)} \mathbb{Z}/2\mathbb{Z} \rightarrow (C_{L,2})^{\Delta}$$

Indeed, $(\sqrt{\beta})$ corresponds to the element $\bigoplus v(\beta)$ in the left hand group so that

$$\ker\phi \cap \bigoplus_{\substack{v \in Ram(L/M) \\ v \neq v_0}} \mathbb{Z}/2\mathbb{Z} = 0.$$

Corollary 25. *Let* $K = \mathbb{Q}(\sqrt{-pq(2+\sqrt{2})})$ *where* p *and* q *are primes such that* $p \equiv -q \equiv 5 \bmod 8$, $\mathcal{P}$ *the prime ideal of* K *above* p *and* $\mathcal{Q}$ *that above* q. *Then the class of* $\mathcal{P}$ (*resp.* $\mathcal{Q}$, $\mathcal{P}Q$) *has order* 2, $C_{K,2}$ *is generated by the classes of* $\mathcal{P}$ *and of* $\mathcal{Q}$. *Also* $\mathcal{P}$ *capitulated in* F_1', $\mathcal{Q}$ *capitulated in* F_2' *and* $\mathcal{P}Q$ *capitulated in* F_3'.

Proof. By the proposition 24, we find that $C_{K,2}$ is generated by the classes of $\mathcal{P}$ and $\mathcal{Q}$.
To show that $\mathcal{P}$ capitulates in $K(\sqrt{p})$, it suffices to see that $\sqrt{p} \in K(\sqrt{p})$ and $(\sqrt{p}^2) = (p)$ in $K(\sqrt{p})$, so $\mathcal{P}$ capitulates in $F_1' = K(\sqrt{p})$ and even $\mathcal{Q}$ capitulated in $F_2' = K(\sqrt{-q})$ and $\mathcal{PQ}$ capitulated in $F_3' = K(\sqrt{-pq})$.

Proposition 26 ([10])**.** *Let* M *a number field contains the m-th roots of unity,* L *a finite extension of* M, $\alpha \in M^*$ *and* $\beta \in L^*$. *We denote by* P *a prime ideal of* M *and* $\mathcal{P}$ *a prime ideal of* L *above* P. *Then*

$$\prod_{\mathcal{P}} \left(\frac{\beta, \alpha}{\mathcal{P}}\right)_m = \left(\frac{N_{L/M}(\beta), \alpha}{P}\right)_m,$$

where the product is taken over all prime ideals of L *which are over* P.

Theorem 27. *Let* $K = \mathbb{Q}(\sqrt{-pq(2+\sqrt{2})})$ *where* p *and* q *are primes such that* $p \equiv -q \equiv 5 \bmod 8$, *then in each extension* F_i', $i \in \{1, 2, 3\}$, *there are exactly two classes of* $C_{K,2}$ *who capitulated and the group* G_2 *is quaternionic of order* 2^m *with* $m > 3$.

Proof. Let ε_0 (resp. ε_2, ε_3) the fundamental unit of $\mathbb{Q}(\sqrt{2})$ (resp. $\mathbb{Q}(\sqrt{p})$, $\mathbb{Q}(\sqrt{2p})$), $\mathcal{P}$ the prime ideal of K above p, $\mathcal{Q}$ that above q, then, by Theorem 18, $\{\sqrt{\varepsilon_0\varepsilon_2\varepsilon_3}, \varepsilon_2, \varepsilon_3\}$ is a fundamental system of units of F_1'.
As $N_{F_1'/K}(\sqrt{\varepsilon_1\varepsilon_2\varepsilon_3}) = \pm\varepsilon_1$ and $N_{F_1'/K}(\varepsilon_2) = N_{F_1'/K}(\varepsilon_3) = -1$, then $E_K = N_{F_1'/K}(E_{F_1'})$. Using the Theorem 4, we find that two Classes only of $C_{K,2}$ capitulate in F_1', namely the class of $\mathcal{P}$ and its square.
By Theorem 19, $\{\xi_3, \xi_5, \xi_7\}$ is a fundamental system of units of F_3'. Since $N_{F_3'/K}(\xi_7) = -1$ and $N_{F_3'/K}(\xi_5) = -N_{F_3'/K}(\xi_3) = \varepsilon_1$, then $E_K = N_{F_3'/K}(E_{F_1'})$,by theorem 4, we find that two classes only of $C_{K,2}$ capitulate in F_3', namely the class of $\mathcal{P}Q$ and its square.
The extension F_1'/K and F_2'/K are of type (B) and the extension F_3'/K is of type (A). Indeed, let $K' = \mathbb{Q}(\sqrt{-q(2+\sqrt{2})})$, then we have $KK' = F_1'$ and as $N_{K/\mathbb{Q}(\sqrt{2})}(\mathcal{P}) = p$ and p is unramified in $K'/\mathbb{Q}(\sqrt{2})$, then to show that $\mathcal{P}$ is inert in F_1'/K, it suffices to show that p is inert in $K'/\mathbb{Q}(\sqrt{2})$ (Translation theorem), For this we compute the norm residue symbol $\left(\frac{p,-q\varepsilon_0\sqrt{2}}{p}\right)$. It has $p \in \mathbb{Q}$ is inert in $\mathbb{Q}(\sqrt{2})/\mathbb{Q}$ and $-q\varepsilon_0\sqrt{2} \in \mathbb{Q}(\sqrt{2})$, so using the proposition 26, we find

$$\left(\frac{p, -q\varepsilon_0\sqrt{2}}{p}\right) = \left(\frac{p, N_{\mathbb{Q}(\sqrt{2})/\mathbb{Q}}(-q\varepsilon_0\sqrt{2})}{p}\right) = \left(\frac{p, 2q^2}{p}\right) = (\frac{2}{p}) = -1,$$

thus p is inert in $K'/\mathbb{Q}(\sqrt{2})$, which gives that $\mathcal{P}$ is inert in F_1'/K and since $[\mathcal{P}]$ is the only nontrivial class of $C_{K,2}$ capitulating into F_1'/K, then F_1'/K is of type (B). Similarly we show that $\mathcal{Q}$ is inert in F_2'/K, which also gives that F_2'/K is of type (B), consequently, by theorem 8, two classes only of $C_{K,2}$ capitulate in F_2'. For F_3', let $L=\mathbb{Q}(\sqrt{2+\sqrt{2}})$, then we have $KL=F_3'$, $N_{K/\mathbb{Q}(\sqrt{2})}(\mathcal{P})=p$ and p is unramified in $L/\mathbb{Q}(\sqrt{2})$, thus to show that $\mathcal{P}$ is inert in F_3'/K, it suffices to show that p is inert in $L/\mathbb{Q}(\sqrt{2})$, for this we compute the norm residue symbol $\left(\frac{p,\varepsilon_0\sqrt{2}}{p}\right)$. Using the proposition 26, we have $p\in\mathbb{Q}$ is inert in $\mathbb{Q}(\sqrt{2})/\mathbb{Q}$ and $\varepsilon_0\sqrt{2}\in\mathbb{Q}(\sqrt{2})$, so

$$\left(\frac{p,\varepsilon_0\sqrt{2}}{p}\right)=\left(\frac{p,N_{\mathbb{Q}(\sqrt{2})/\mathbb{Q}}(\varepsilon_0\sqrt{2})}{p}\right)=\left(\frac{p,2}{p}\right)=(\frac{2}{p})=-1,$$

thus p is inert in $L/\mathbb{Q}(\sqrt{2})$, which gives that $\mathcal{P}$ is inert in F_3'/K, similarly one shows that $\mathcal{Q}$ is inert in F_3'/K. As $\mathcal{P}\mathcal{Q}$ capitulated in F_3', then by applying the reciprocity law of Artin, we find that F_3'/K is of type (A). Consequently, using theorem 8, the group G_2 is isomorphic to Q_m with $(m>3)$. $\square$

Example 28. *Let* $K=\mathbb{Q}(\sqrt{-55(2+\sqrt{2})})$, $F_1'=K(\sqrt{5})$, $F_2'=K(\sqrt{-11})$ *and* $F_3'=K(\sqrt{-55})$, *then by theorem* 27 *in each extension* F_i', $i\in\{1,2,3\}$, *there are exactly two classes of* $C_{K,2}$ *who capitulated and the group* G_2 *is quaternionic of order* 2^m *with* $m>3$.

Remark 29. *Let* $K=\mathbb{Q}(\sqrt{-pq(2+\sqrt{2})})$ *and* $K_0=\mathbb{Q}(\sqrt{2},\sqrt{-pq})$ *where* p *and* q *are primes such that* $p\equiv -q\equiv 5 \bmod 8$, *then* $\#\, G_2=4\,h_2(K_0)$.

Proof. We have $K_2^{(1)}/F_3'$ unramified extension and as F_3'/K is of type (A), then, according to [14], $C_{F_3',2}$ is cyclic, so F_3' and $K_1^{(2)}$ has even Hilbert 2-class field, namely $K_2^{(2)}$, so $\#\, G_2=2\,h_2(F_3')$. Moreover $F_3'/\mathbb{Q}(\sqrt{2})$ is a normal biquadratic extension of Galois group of type $(2,2)$ and sub-quadratic extensions K, K_0 and $L=\mathbb{Q}(\sqrt{2+\sqrt{2}})$, by [16], we show that

$$h_2(F_3')=\frac{1}{2}q(F_3'/\mathbb{Q}(\sqrt{2}))h_2(K)h_2(K_0)h_2(L),$$

and since $h_2(K)=4$, $q(F_3'/\mathbb{Q}(\sqrt{2}))=1$ and $h_2(L)=1$ (see [24]), then $h_2(F_3')=2\,h_2(K_0)$, which gives $\#\, G_2=4\,h_2(K_0)$. $\square$

Corollary 30. *Let* $K=\mathbb{Q}(\sqrt{-pq(2+\sqrt{2})})$ *where* p *and* q *are primes such that* $p\equiv -q\equiv 5 \bmod 8$ *and* $(\frac{p}{q})=-1$, *then in each of the extensions* F_i', *for* $i\in\{1,2,3\}$, *there are exactly two classes of* $C_{K,2}$ *which capitulated and* $G_2\simeq Q_4$. *Moreover, the* 2*-class group of* F_3' *is cyclic of order* 8, *and the* 2*-class groups of* F_2' *and* F_1' *are of type* $(2,2)$.

Proof. Since $p\equiv -q\equiv 5 \bmod 8$, then, by Theorem 27, G_2 is quaternionic of order 2^m with $m>3$. Let $K_0=\mathbb{Q}(\sqrt{2},\sqrt{-pq})$, since $(\frac{p}{q})=-1$, then, according to [17], we have $h_2(K_0)=4$, by the remark 29, we find that $G_2\simeq Q_4$ and the 2-class group of F_3' is of order 8. So the 2-class group of F_3' is cyclic of order 8, and the 2-class groups of F_2' and F_1' are of type $(2,2)$. $\square$

Example 31. *Let* $K=\mathbb{Q}(\sqrt{-15(2+\sqrt{2})})$, $F_1'=K(\sqrt{5})$, $F_2'=K(\sqrt{-3})$ *and* $F_3'=K(\sqrt{-15})$, *then by corollary* 30 *in each extension* F_i', $i\in\{1,2,3\}$, *there are exactly two classes of* $C_{K,2}$ *who capitulated. Moreover, in this case, the* 2*-class group of* F_3' *is cyclic of order* 8 *and the* 2*-class groups of* F_1' *and* F_2' *are of type* $(2,2)$ *and* G_2 *is quaternionic of order* 16.

References

[1] A. Azizi, *Capitulation des 2-classes d'idéaux de $\mathbb{Q}(\sqrt{d}, i)$,* C.R.A.S. Paris, t. **325**, série I, (1997), 127-130.

[2] A. Azizi, *Unités de certains corps de nombres imaginaires et abéliens sur $\mathbb{Q}$,* Ann. Sci. Math. Québec **23** (1999), 87-93.

[3] A. Azizi, *Capitulation des 2-classes d'idéaux de $\mathbb{Q}(\sqrt{2pq}, i)$,* Acta Arithmetica **94** (2000), 383-399.

[4] A. Azizi, *Sur une question de Capitulation,* Proc. Amer. Math. Soc. 130 (2002), 2197-2002.

[5] A. Azizi, *Sur les unités de certains corps de nombres de degré 8 sur $\mathbb{Q}$,* Ann. Sci. Math. Québec **29** (2005), 111-129.

[6] A. Azizi et M. Talbi, *Capitulation des 2-classes d'idéaux de certains corps biquadratiques cycliques,* Acta Arithmetica **127** (2007), 231-248.

[7] A. Azizi et M. Talbi, *Capitulation dans certaines extensions non ramifiées de corps quartiques cycliques,* Archivum Mathematicum (BRNO) **44** (2008), 271-284.

[8] E. Brown and C. J. Parry, *The 2-class group of certain biquadratic number fields II,* Pacific Journal of Mathematics, Vol. **78**, **No**. 1, (1978), 11-26.

[9] P. E. Conner and J. Hurrelbrink, *Class number parity,* Series in Pure Mathematic, World Scientific, (1988).

[10] H. Hasse, *Neue Begründung der Theorie des Normenrestsymbols,* J. Reine Angew. Math. **162** (1930), 134-143.

[11] F. P. Heider, B. Schmithals, *Zur Kapitulation der Idealklassen in unverzweigten primzyklischen Erweiterungen,* J. Reine Angew. Math. **366** (1982), 1-25.

[12] M. Ishida, *The genus fields of algebraic number fields,* Lecture notes in mathematics 555, Springer-Verlag (1976)

[13] P. Kaplan, *Sur le 2-groupe des classes d'idéaux des corps quadratiques,* J. Reine Angew. Math. **283/284** (1976), 313-363.

[14] H. Kisilevsky, *number fields with class number congruent to 4 modulo 8 and Hilbert's theorem 94,* J. Number Theory **8** (1976), 271-279.

[15] S. Kuroda, *Über den Dirichletschen Zahlkörper,* J. Fac. Sci. Imp. Univ. Tokyo Sec. I, **4** (1943), 383-406.

[16] F. Lemmermeyer, *Kuroda's class number formula,* Acta Arith. **66** (3) (1994), 245-260.

[17] T. M. McCall, C. J. Parry and R. R. Ranalli *Imaginary bicyclic biquadratic fields with cyclic* 2*-class group,* Journal of Number Theory **53** (1995), 88-99.

[18] K. Miyake, *Algebraic Investigations of Hilbert's Theorem* 94*, the Principal Ideal Theorem and Capitulation Problem,* Expos. Math. 7 (1989), 289-346.

[19] P. J. Sime, *On the ideal class group of real biquadratic fields,* Trans. Am. Math. Soc. 347, No. 12,4855- 4876(1995).

[20] H. Suzuki, *A Generalisation of Hilbert's Theorem 94,* Nagoya Math. J., vol 121 (1991).

[21] H. Suzuki, *On the Capitulation Problem: Class Field Theory, Its Centenary and Prospect*. Adv. Stud. In Pure Math. 30. Math. Soci. of Japan, Tokyo 2000.

[22] O. Taussky, *A Remark on the Class Field Tower*. J. London Math. Soc. 12 (1937), 82-85.

[23] H. Wada, *On the class number and the unit group of certain algebraic number fields,* Tokyo U. Fac. of Sc. J., Serie I, **13** (1966), 201-209

[24] L. C. Washington, *Introduction to cyclotomic fields,* Graduate texts in mathematics **83** (1996).

Synthesis and UV-Visible complexation study of 1-pyrazolylbenzimidazol-2-one polyether macrocyclic derivatives

Joseph Nathan Tené Ghomsi,[1] Rachid Bouhfid,[2] Noureddine Hamou Ahabchane,[1]
El Mokhtar Essassi[1,2,*]

[1] Laboratoire de Chimie Organique Hétérocyclique, URAC 21, Pôle de Compétences Pharmacochimie,Université Mohammed V- Agdal, Avenue Ibn Battouta, BP 1014, Rabat, Morocco
[2] Centre Composites Nanocomposites, Moroccan Foundation for Advanced Science, Innovation and Research (MAScIR), Rabat Design Center, Rue Mohamed Al Jazouli
Madinat Al Irfane, Rabat 10100, Morocco
* Corresponding Author E-mail: emessassi@yahoo.fr

Abstract. *A new polyether macrocyclic of 1-pyrazolylbenzimidazol-2-ones* **5-6** *have been synthesized by the reaction of dichloro(poly)ethylene glycol in phase transfer catalysis conditions. The structure of these compounds were identified by ^{1}H NMR, ^{13}C NMR, IR spectroscopy and Mass spectrometry. The formation of Li^+, Na^+, and K^+ complexes with compounds* **5-6** *has been investigated by UV-visible spectroscopy. It was demonstrated that ligand 5 form preferential complex with Li^+ cation.*

Key words: synthesis,complexation,ligand,1-(3'-phenylpyrazol-5'-yl)benzimidazolo-13(15)-couronne-2(3).

1. Introduction

The development of new molecular models for recognition, titration and transport of metals is an area of research that has grown considerably since the discovery of crown ethers [1]. Although some examples of macrocyclic polyethers have been described in the literature before the work of Pedersen, and highlighting their ability to complex metals.

Based on these compounds Lehn (Nobel Prize in Chemistry in 1987) introduced the concept of a new interdisciplinary chemistry (physics, chemistry and biology), based on non-covalent intermolecular bonds (Van der Wals force, repulsion at short distance, electrostatic bonding, and hydrogen bonding): supramolecular chemistry [2]. This chemistry has grown in recent years, mainly in order to develop systems able to complex metal cations [3-5]. The ability of these macrocycles to form complexes with metals allowed their use in various areas: in medicine, they are involved in the transport of ions across a membrane. Hemoglobin, for example, which is involved in the transport of oxygen in the body is a complex iron atom bonded to four nitrogen atoms donor cycle consists of porphyrine. To fight against certain deficiencies metals are introduced into the body as a complex, in excess, it uses a powerful ligand [6,7]. In the chemical industry, the complexes of transition metals act as catalysts [8], which are involved in the construction of ion-selective electrodes [9]. They are also used as photosensitizing agents in the conversion of solar energy. In addition, we are all aware of the dangers of rejection in the nature of industrial heavy metals. Acid rain burn leaves and fish poison, killing most, if not all, aquatic wildlife, where the interest for ligands capable to complex very selectively these metals to their use for protection environment.

The aim of this work is the synthesis of new ligands containing in their structure benzimidazole, pyrazole and polyether macrocycle and the study of their complexation with alkali metals by UV-Visible spectroscopy.

2. Results and Discussion

2.1. Synthesis and characterization

In order to prepare a new polyether macromolecules incorporating a benzimidazole and pyrazole nucleus, we have chosen as synthetic substrate the 1-pyrazolylbenzimidazol-2-one **2**, obtained by the action of ethyl chloroformate to 3 (5) -*N*-(*o*-aminophenyl) aminopyrazole **1** in pyridine at 80°C for 24 hours. (Scheme 1). [10]

The obtained 1-pyrazolylbenzimidazol-2-one **2** was reacted with dichloropolyethylene glycols **3a**-**c** freshly prepared by the action of thionyl chloride on dihydroxylypolyethylene glycol in benzene in the presence of a catalytic amount of pyridine. [11]

Condensation of these reagents, in stoichiometric amount or in excess to 1-pyrazolylbenzimidazol-2-one **2** is carried out under the phase transfer catalysis conditions in the presence of potassium carbonate K_2CO_3 under magnetic stirring at 80 °C. The results obtained depend on the chain length of polyethylene glycol used.

Indeed, when using dichlorodiethylene glycol **3a**, the reaction does not lead to the cyclised product, but to the compound **4**, resulting in two monoalkylations, one on the nitrogen atom of the benzimidazole ring and the other on the pyrazole nitrogen. The use of the spacer **3a** does not allow to obtain polyether macrocycles probably due to the length of the chain. To overcome this problem, we used the dichlorotriethylene glycol **3b** with more ethyleneoxy spacer in the same conditions as the first reaction (Scheme 1).

The reaction in this case,led to the formation of the 1-pyrazolylbenzimidazolo 13 courone-2 **5**, resulting from the cyclization [1+1]. The chain links polyether with pyrazole and benzimidazole nitrogens.

In the light of these results, we used the dichlorotetraethylene glycol **3c** having a longer chain, which can lead to new macrocycles containing one or two pyrazolylbenzimidazolones units. However, the reaction gives a new macrocycle **6**, resulting from the cyclization [1+1] larger than the previous cavity.

The structure of obtained compounds were confirmed by ^{1}H NMR, ^{13}C NMR, mass spectrometry and by X-ray crystallographic study.

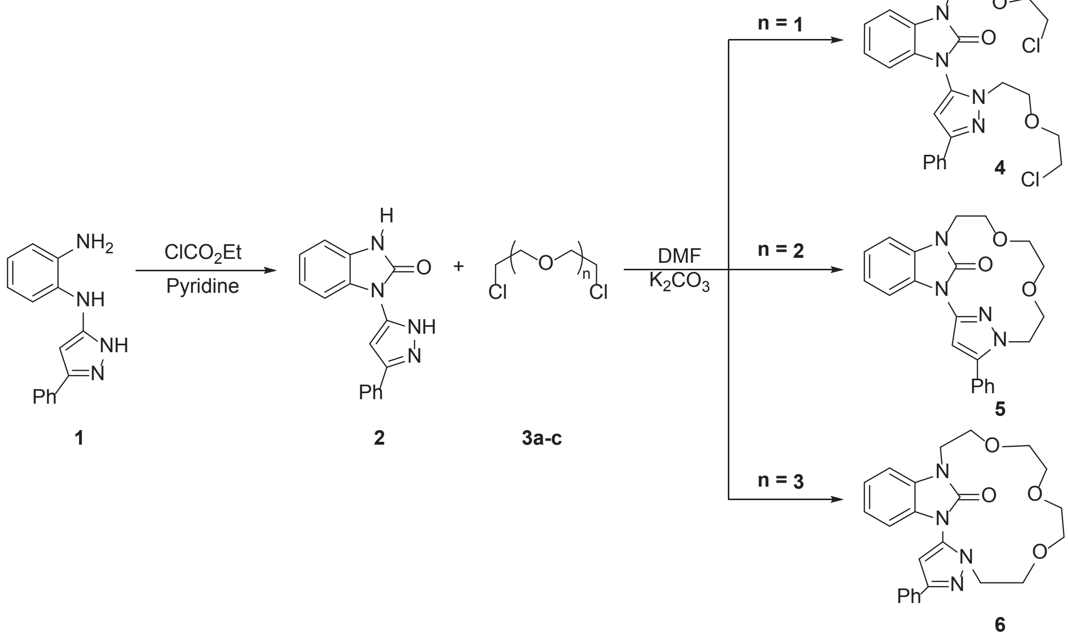

Scheme 1.

The IR spectrum of compound **2** shows, the characteristics absorption bands of the NH groups of pyrazole and benzimidazole at 3250 and 3325 cm^{-1} respectively and the absorption of the carbonyl band at 1710 cm^{-1}.

The ^{1}H NMR spectrum shows particularly, in addition to the signal at 6.97 ppm due to the proton at position 4 of the pyrazole ring; the signals related to aromatic protons form a multiplet between 7.24 and 7.75 ppm. In the ^{13}C NMR spectrum, it is noted, in particular, the presence of a signal at 96.01 ppm, attributed to the carbon at the position 4 of the pyrazole [20].The mass spectrum (EI) shows the molecular ion peak at m / z = 276.

The ^{1}H NMR spectrum of compound **4**, shows the signals due to the methylene protons as multiplet between 3.25 and 4.29 ppm. The signal of the pyrazole proton in position 4 appears at 6.66 ppm. In its ^{13}C NMR spectrum is observed, in particular, the eight signals of the methylene groups, two of them are linked to benzimidazole and pyrazole nitrogen (41.93 and 49.25 ppm), four are linked to oxygen atoms (from 71.46 to 68.82 ppm) and the two attached to chlorine atoms (42.62 ppm). The carbon at position 4 of the pyrazole resonates at 100.83 ppm, while the aromatic carbons give resonance signals between 128.73 and 108.1 ppm. In mass spectrum (EI), the peak of the molecular ion (m / z = 488 corresponding to the formula $C_{24}H_{26}N_4O_3Cl_2$) with isotope profile characteristic of the presence of two chlorine atoms.

The IR spectrum is characterized by an absorption band at 1695 cm^{-1}, relative to the C=O. It is noted the disappearance of a broad absorption band around 3200 cm^{-1} which demonstrates the alkylation of NH groups, and the presence of intense bands between 2800 and 3000 cm^{-1} due to the different groups of the ether methylene chain.

The ^1H NMR spectrum compound **5**, exhibits the pyrazole proton signal at 6.81 ppm, and the signals related to the 12 methylene protons appearing as multiplet between 3.15 and 4.51 ppm. The massive between 6.84 and 7.83 is assigned to the resonance of the aromatic protons.

The ^{13}C NMR spectrum shows all signals of methylene carbons: those linked to oxygen atom give signals between 66 and 71 ppm, while those attached to nitrogen appear between 40 and 50 ppm. The deshielded signal at 151.17 ppm confirms the non-participation of the C=O function to cyclization. This is also confirmed by an examination of its IR spectrum showing an absorption band around 1700 cm^{-1}. The absence of absorption bands related to NH groups reveals their involvement in the reaction. The mass spectrum obtained using ammonia as the reagent gas, shows the peak of this pseudo-molecular ion at 391, corresponding to the macrocycle cyclization [1+1]. The peak at 408 corresponds to $[M+NH_4]^+$.

The ^1H NMR spectrum of compound **6** shows, in particular, all the signals due to six methylene protons as a multiplet between 2.76 and 4.53 ppm. The pyrazole proton resonates at 6.65 ppm, while the signals related to aromatic protons were observed between 6.86 and 7.82 ppm. In the ^{13}C NMR, we note the presence of signals assigned to the carbon sp^3 methylene groups bonded to oxygen and nitrogen atoms appearing at 40.43, 51.71 and 66.45 to 70.42 ppm. The carbon in position 4 of the pyrazole and the C=O resonate respectively at 103.16 and 153.99 ppm. The mass spectrum, also obtained by the DIC mode (reactant gas: ammonia), exhibits the peak of the protonated molecular ion at 435 corresponding to the molecular formula $C_{24}H_{26}N_4O_4$ macrocycle. The peak at 452 corresponds to $[M+NH_4]^+$.

A crystallographic study [12] of compound **6** confirmed its structure, resulting from involvement in the macrocyclization reaction of the benzimidazole nitrogen and nitrogen pyrazole nucleus (figure 1).

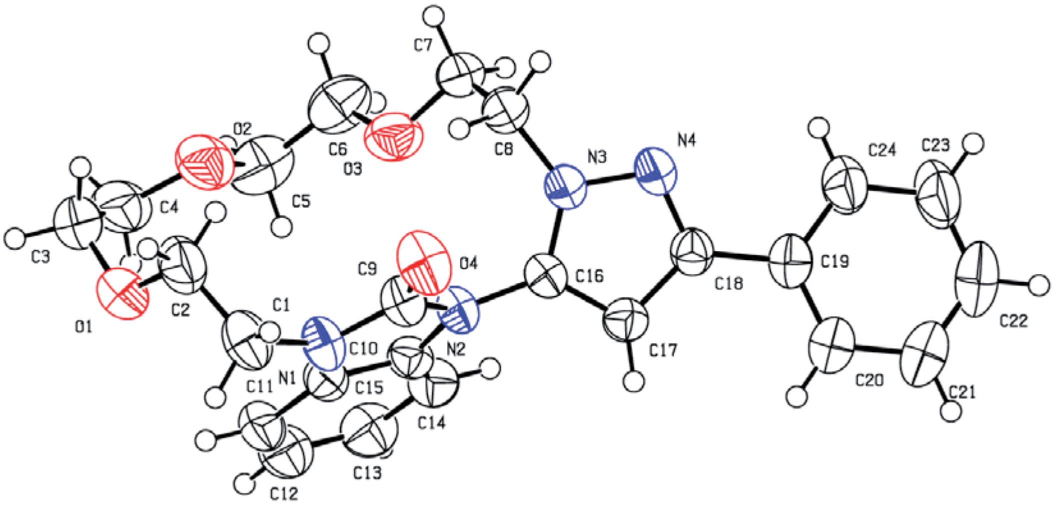

Figure 1 :ORTEP diagram of $C_{24}H_{20}N_4O_4$ with 50% probability ellipsoids.

2.2. Synthesis and characterization

The stability constants were measured in THF solutions by UV-visible spectrophotometry for ligands /metallic picrate complexes. This technique is particularly suitable for the measurement of stability constants ranging from 10^2 to 10^5 l.mol^{-1}.

The UV-Visible spectrum of ligand **5** has a main absorption band at λ = 258 nm (ε = 27237 cm^{-1}mol^{-1}). The observed band in this ligand is probably due not only to the interactions between chromophores, but also transitions $\pi \rightarrow \pi^*$.

the complexation of 1-pyrazolylbenzimidazolo-16-crown-3 **6** with alkali metallic picrates (Li^+, Na^+ and K^+) in THF showed no wavelength shift and no isosbestic point allowing to confirm that no complex has been formed.

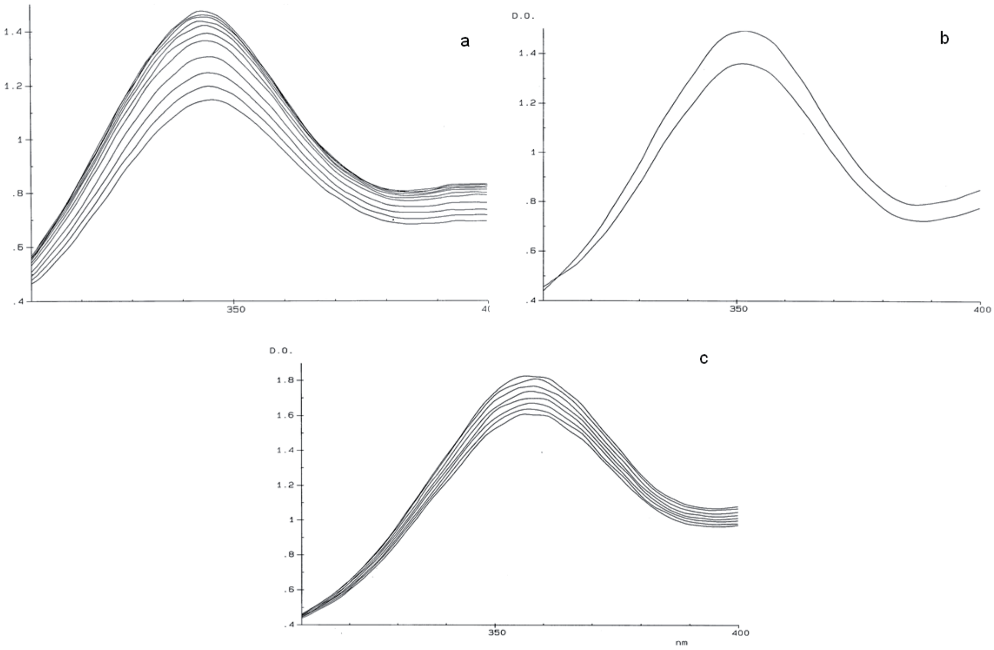

Figure 2. Absorption spectra: a- PicLi$^+$in THF after addition of **<u>6</u>**; b- PicNa+ in THF after addition of **<u>6</u>**; c-PicK+ in THF after addition of **<u>6</u>**.

The effect of cavity size of chelating properties of 1-pyrazolylbenzimidazolo-13-couronne-2 **<u>5</u>**, have been studied.

The UV-visible spectrum of ligand **<u>5</u>** presents the main absorption band at λ = 250 nm (ε = 29125 $cm^{-1}mol^{-1}$). The table 1 shows the experimental variation of the wavelength λ_{max} of metal picrate as function of amount of ligand added. (ρ)

<u>Table 1</u> : Value of λ_{max} = f(ρ)

Metal Picrates	λ_{max}, ε ρ = 0	λ_{max}, ε ρ = 20	$\Delta\lambda_{max}$
PicLi	345 ; 14079	372 ; 12189	27
PicNa	352 ; 16550	370 ; 14967	18
PicK	357 ; 17917	372 ; 16166	15

According to this table, the addition of the ligand, non-absorbent between 300 and 400 nm, resulting in a significant shift of the wavelength. This displacement decreases when going from lithium (r = 0.78 Å) to potassium (r = 1.33 Å) is certainly due to the phenomenon of complexation.

The analysis of the evolution of spectra showing the variation of λ_{max} reveals a bathochromic and hyperchromic band of picrates ions. All these curves (obtained by ISOBEST) pass through the isosbestic point. These points are located at: 355 nm for complex **5**/Li$^+$,358 nm for complex **5**/Na$^+$, and 360 nm for complex **5**/K$^+$

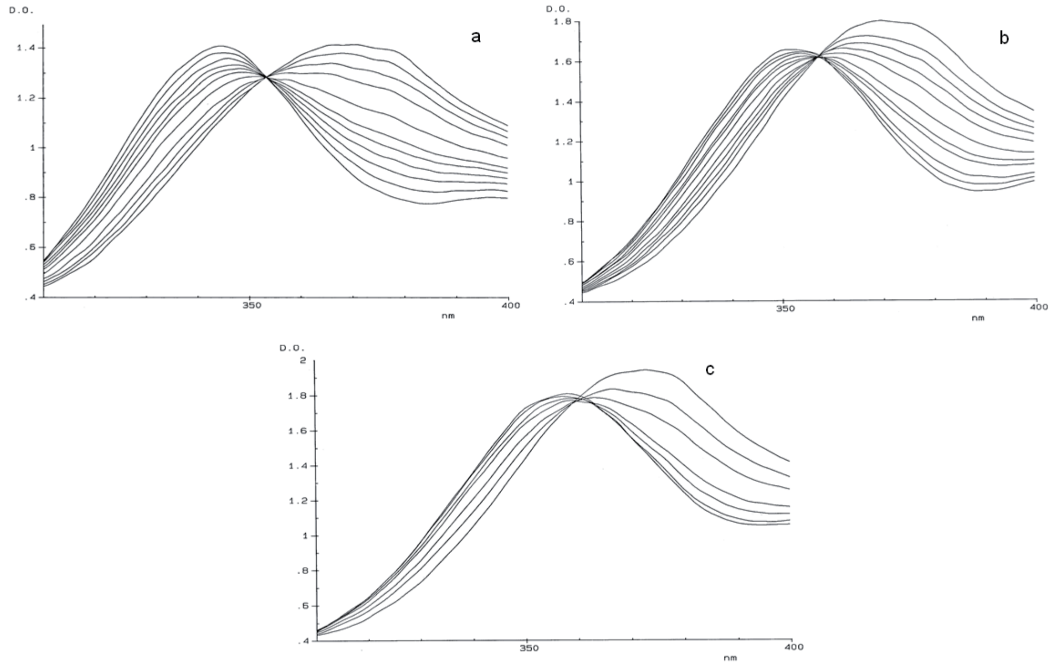

Figure 3. Absorption spoectra of : a- PicLi$^+$ in THF after addition of **5** ; b- PicNa$^+$ in THF after addition of **5** ; c-PicK$^+$ in THF after addition of **5**

The evolution of species according to ρ (ρ = [L] / [M]) of **5**/Li complex is given in Figure 3.

The examination of this figure shows that the complex formed is not stable (log K < 3). Indeed in the case of strong complexes, and the curve of the metal complex intersect at a isobestic point , so that when the complex is instable. Such is the case for the complex formed between **5** and Na$^+$ and K$^+$ (Figure 3).

Table 2 : stability constante of Li^+, Na^+ and K^+ complexes

		log β	
Complexe	$\rho = n_L / n_M$	ML	$S(A) \leq 0{,}005$
5/Li^+	$0 \leq \rho \leq 20$	2,40 ± 0,1	0,002
5/Na^+	$0 \leq \rho \leq 20$	2,04 ± 0,1	0,0041
5/K^+	$0 \leq \rho \leq 20$	1,9 ± 0,1	0,0051

The optimization of geometry of the complex led us to a modeling study of the complex using the molecular mechanics software InsightII. From this study, it appears that the three oxygen atoms of the ligand involved in ML complex. The Li-O distances are very short, that confirm the stability of complex with lithium ion. The distances are as follows:

- Li-O ether (pyrazole side): 1.92 Å
- Li-O ether (imidazole side): 1.91 Å
- Li-C=O: 1.81 Å.

The structure of the complex is presented by the following figure:

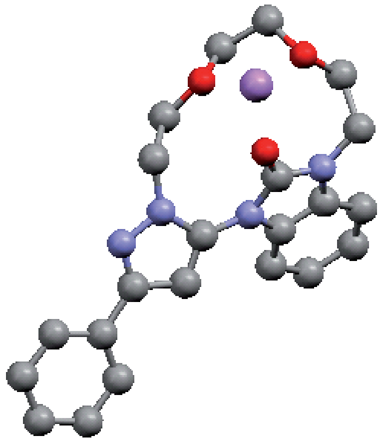

Figure 4. Modeled structure of the complex ML of 5/Li

3. Conclusion

In this work, a novel polyether macrocyclic we explored by UV spectrophotometry, the complexing properties of the two macrocycles prepared in our laboratory, towards metal picrates. According to this technique, it appears that the macrocycle **6** could not complex any metal cation among those, which were tested, while the ligand macrocycle **5** was able to complex selectively the lithium cation. This could be useful in clarifying the mechanism by which lithium is incorporated into the biological system because this metal known current medical applications of particular interest in the medical world. [13]

4. Experimental part

Melting points were determined with a Buchi-Tottoli apparatus and are uncorrected. Infrared spectra were recorded on a Perkin-Elmer 1600 spectrophotometer in KBr disks. NMR spectra were recorded on a Bruker AC 250 spectrometer, 1H (250 MHz) and 13C (62.89 MHz) and are reported in parts per million. Data are reported in the following order: chemical shift, spin multiplicity (s = singlet, d = doublet, t = triplet, m = multiplet), coupling constant, integration and assignment. UV-Vis spectra were monitored on a Perkin-Elmer Lambda 17 spectrophotometer coupled with an Epson PC AX Elmer computer. The mass spectra were recorded on a Varian Mat 311A for (EI) or by (DCI, NH_3).

Preparation of 1-(3’-phenylpyrazol-5’-yl)benzimidazol-2-one 1

To a solution of 3(5)-*N*-(*o*-aminophenyl) aminopyrazole(0.01 mole) **1** in 40 ml of pyridine, was added ethyl chloroformate(0.05 mole)and refluxed for 6 hours. After cooling, the pyridine was removed under vacuum, and the residue obtained was recrystallized from water-ethanol.

Yield: 80 %

Mp: more than 260 °C

^{1}H NMR ($CDCl_3$ + CF_3CO_2H): 6,97 (s, 1H, C_4H); 7,24-7,75 (m, 9H)

^{13}C NMR ($CDCl_3$ + CF_3CO_2H): 96,01 (=C_4H); 117,69-131,62 (CHar); 126,48 (Car); 126,88 (Car); 127,47 (Car); 139,79 (Cq); 147,83 (C=N); 153,88 (C=O)

Mass spectrometry DCI (NH_3): $[M+H]^+$: 277.

General method for preparation of compounds 4, 5 and 6:

To a solution of 1-(3-phenylpyrazolyl)benzimidazol-2-one (0.01 mole) in 60 mL of N,N-dimethylformamide, 0.02 mole of dichlorodiethylene glycol (dichlorotriethylene glycol and dichlorotetraethylene glycol), 0.04 mole of potassium carbonate and 0.001 mole of tetra-n-butylammonium bromide were added. The mixture was stirred at 80°C for 24hours. Then insoluble salts were filtred off and the solvent was evaporated in vacuum. The residue was separated by gel silica chromatography.

1-[(1’-chlorodiethyleneglycol-3’-phenyl)pyrazol-5’-yl]-3-chlorodiethyleneglycol benzimidazol-2-one 4

Yield: 38 %

Mp: 106-108 °C

^{1}H NMR ($CDCl_3$) : 3,25 (m, 16H) ; 6,66 (s, 1H) ; 6,81-7,8 (m, 9H)

^{13}C NMR ($CDCl_3$) : 41,29 (CH_2Cl); 41,64 (CH_2Cl); 42,44 (NCH_2); 42,89 (NCH_2); 49,27 (OCH_2); 69,2 (OCH_2); 69,6 (OCH_2); 71,22 (OCH_2) ; 100,83 (=C_4H); 108,1-128,73 (CHar); 129,61 (Car); 130,19 (Car); 133,13 (Car); 133,77 (Cq); 151,17 (C=N); 152,81 (C=O)

Mass spectrometry EI : (m/z): 488.

1-(3'-phenylpyrazol-5'-yl)benzimidazolo-13-couronne-2 5

This compound was obtained as white powder after a silica column chromatography using as eluant (Hexane/ethyl acetate: 6/4)

Yield: 33%

Mp: 174-176 °C

^{1}H NMR ($CDCl_3$) : 3,15-3,52 (m, 4H); 3,71-3,95 (m, 5H); 4,06-4,19 (m, 1H); 4,42-4,61 (m, 2H); 6,81 (s, 1H); 6,84-7,83 (m, 9H)

^{13}C NMR ($CDCl_3$) : 40,43 (NCH_2); 51,71 (NCH_2); 66,45 (OCH_2) ; 70,12 (OCH_2) ; 70,32 (OCH_2) ; 70,42 (OCH_2) ; 103,16 (=C_4H); 108,54-128,72 (CHar); 129,14 (Car); 129,46 (Car) ; 129,89 (Car); 133,15 (Cq); 150,65 (C=N); 153,99 (C=O)

Mass spectrometry DCI (NH_3): $[M+H]^+$: 391.

1-(3'-phenylpyrazol-5'-yl)benzimidazolo-16-couronne-3 6

This compound was obtained as white crystal after silica column using eluant (Hexane/ethyl acetate: 7/3)

Yield: 25%

Mp: 129-131 °C

^{1}H NMR ($CDCl_3$) : 2,76 (m, 1H) ; 3,26-3,46 (m, 6H) ; 3,7-398 (m, 6H) ; 4,31-4,53 (m, 3H); 6,65 (s, 1H) ; 6,66-7,83 (m, 9H)

^{13}C NMR ($CDCl_3$) : 41,22 (NCH_2); 50,96 (NCH_2); 69,02 (OCH_2); 69,94 (OCH_2); 70,07 (OCH_2); 70,29 (OCH_2); 100,99 (=C_4H); 106,49-128,55 (CHar); 130,04 (Car); 129,74 (Car); 129,98 (Car); 133,21 (Cq); 150,94 (C=N); 152,55 (C=O)

Mass spectrometry DCI (NH_3): $[M+H]^+$: 435

Determination of formation constants.

The formation constants for ion-ligand complexes were determined by UV spectrophotometry in tetrahydrofuran solutions following Smid. [14-15] The sequential addition of aliquots of a ligand to a $3x10^{-5}$M solution of metal picrate in THF (ρ = ligand/sait = 0 to 10-17) induces large spectral changes in the 280-450 nm wavelength range. The calculation method uses the STAR/FA and the STAR programs developped by Beltran [16] for studying ionic equilibrium from spectrophotometric data. STAR is a non-linear regression program for the refinement of complex formation constants. The mass balance equations of the system were solved from the given model and the total concentration of the components. STAR gives several statistical characteristic parameters to test the reliability of the regression process. The most important parameter is the standard deviation of the absorbances (A) which must be compared to the instrumental error of the spectrophotometer 0.002; an acceptable fit is $S(A) < 0.005$. Other parameter: the distribution of residuals is examined by the Skewness, Kurtosis and Pearson's χ^2 tests; for a Gaussian distribution these values should be equal to 0.3 and < 12.6 (for six degrees of freedom at the 95% confidence level) respectively. The Hamilton R factor(%) indicates the relative fit (SI%). The STAR/FA program is used to determine the number of absorbing species in solution by factor analysis of the absorbance data matrix. In all cases the characteristic parameters were very good.

References

[1] C.J. Pedersen, J. Am. Chem. Soc., 89 (1967), 2495, 7017.

[2] J.M. Lehn, La chimie supramoléculaire, concepts et perspectives, Trad. par André Pousse, Paris-Bruxelles (1997).

[3] Van Veggel, M. Bos, S.Harkema, H. Van de Bovekang, W. Verboo et D.N. Reinhould, J. Org. Chem., (1991), 56, 225.

[4] G.L. Rothermel, Jr. Lain Miao, A.L. Hill et S.C. Jackets, Inorg. Chem., (1992), 31, 4854.

[5] A. Basak and J. Chandra Shain, Tetrahedron Lett., 39, 3029 (1998).

[6] R. Izatt, G.L. Lindh, G.A. Clark, Y. Nakatsuji, J.S. Bradshaw, J.D. Lamband, J.J. Christensen, J. Memb. Sci., (1987), 31.

[7] A.M. Costero et S. Rodriguez, Tetrahedron Lett., (1992), 33, 623.

[8] C.M. Starks et Liotta, Phase Transfer Catalysis, Academic Press, New York (1978).

[9] O. Ryba et Petranek, J. Electroanal. Chem. Interf. Electrochem., (1973), 44, 423.

[10] M. J. Kornet, T. Masaru, J. Heterocyclic Chem., 21, 1533 (1984).

[11] B. P. Czech, A. Czech, B. Son, H. K. Lee et R. A. Bartsch, J. Heterocyclic Chem., 23, 465

[12] J.N.Ghomsi,R.Bouhfid,N.H.Ahabchane,E.M. Essassi,S.W.Ng,Acta Cryst. (2009), E65,o 2493

[13] R. O. Bach, Lithium- Curent Applications in Science, Medicine and technology, Wiley-Interscience, New York (1985).

[14] Wong, K.H.; Bourgoin, M.; Smid, J. J. Chem. Sot., Chem. Commun. (1974), 715.

[15] Bourgoin, M.; Wong, K.H.; Hui, J.Y.; Smid, J. J. Am. Chem. Sot. (1975), 97, 3462.

[16] Beltran, J.L.; Codony, R.; Prat, M.D. Anal. Chim. Actu (1993),276, 441.

Atomic relaxation of Ag and Cu on fcc(100) and (110) surfaces

K. Sbiaai [1,*], M. Mazroui [2], K. Benkhouja [3], Y. Boughaleb [2,4,5,]**

[1]Univ. Hassan 1, Faculté polydisciplinaire de Khouribga, 26000 Settat, Morocco.
[2]Laboratoire de Physique de la Matière Condensée, Unité de recherche associée au CNRST (URAC 10), Université Hassan II- Mohammedia. Faculté des Sciences Ben M'Sik, B.P. 7955, Casablanca, Morocco.
[3]Equipe des Matériaux, Nanomatériaux, Eau et Dessalement (EMNED), Université Chouaib Doukkali, Faculté des sciences, El Jadida, Morocco
[4] Ecole Normale Supérieure, Université Hassan II, Casablanca, Morocco.
[5] Hassan II Academy of Science and Technology, Rabat, Morocco

Corresponding authors: (*) ksbiaai@gmail.com, (**) yboughaleb@yahoo.fr

Abstract *In this work we investigated the atomic relaxation in copper and silver substrates. The system surfaces are oriented following (100) and (110) directions. The relaxation and the bond length variation are only obtained by the mutual atomic interaction. The all calculations are made at zero Kelvin in order to neglect the thermic vibration of the substrate atoms. The (100) surfaces are more compact than (110) ones, which is clearly observed in the inter-layer relaxation rate. On the other hand, the investigation of the adatom relaxation in the case of heterosystems (Cu/Ag) reveals that Cu adatom tends to penetrate through the surface which corresponds to the exchange process. In contrast, the Ag adatom on Cu surface attempts to be far from the surface giving a preferential occurrence to the jump process on the surface. This finding is confirmed by the binding strength or binding energy calculations where we have found (for (100) surface as example) that Cu-Ag is 2.30 and 2.09 eV for Cu/Ag and Ag/Cu, respectively.*

Key words: atomic relaxation, mutual interaction, copper and silver, Embedded Atom model, Dynamic molecular simulation.

1. Introduction

There exists a wide variety of applications of thin films such as optoelectronic devices and micro-semiconductors. Due to this importance, the thin film growth has been the subject of many investigations over the last decade. In this context, understanding of epitaxial process including diffusion phenomena, leads to the amelioration of material performance. For this reason, the description of thin films growth needs a total understanding of different based elements which could control the diffusion phenomena.

The studies of the ultra-thin film kinetics start from the first based diffusion elements such as adatoms. Many investigations are made in order to extract the different diffusion processes which could exist during adatom diffusion. However, the study of the atomic structure relaxation is a very important element in the growth thin film phenomena. Such investigation leads to the prediction of the most stable structure during the epitaxial phenomenon.

Using theoretical modeling, it has been demonstrated that adatom diffusion could occur via simple jump, long jump or exchange phenomena [1-5]. However, all of these processes have been revealed by experimental tools [6.7].The adatom diffusion on metallic surface, especially on low Miller index surfaces, has been studied in several previous works [8,9]. Attention has also been paid to evaluations of the heteroepitaxial growth investigation until now [8-10], and the phenomenon which could be met during this process still needs more detailed understanding. In this way, the two heterosystems Ag/Cu(100) and Cu/Ag(100) are studied in previous work using *ab* initio tools [2]. It has been shown that the bond length relaxation in the presence of adatoms differ from one system to another. This difference leads to a first prediction of adatoms diffusion processes on the surface either on terrace (perfect surface) or near the step edge. For example, in the case of Cu/Ag(100), the investigation of bond length relaxation and binding energy demonstrates that the adatom tends to diffuse via a mechanism more complicated than the jump one[2]. On the other hand, one knows that the activation energy or potential barrier (the energy which the adatom has to overcome for making the jump) is strongly related to the number and the strength of the bonds between adatom and their first neighbors.

Our aim in this work is to calculate the bending energy between adatom and substrate atoms, especially those rounding the adatom adsorption position. We have also examined the adatom influence on atoms substrate relaxation. This investigation allows us to understand adatom behavior in the case of heterogeneous systems both in the case of (100) and (110) surface for copper and silver materials. Following this way, we have calculated the reduced distance between adatom and surface after relaxation process. We have chosen (100) and (110) tailored from face centered cube (fcc), where the adatom has the same number of the first nearest neighbors but with difference in the geometry of adsorption position (square for (100) and rectangular for (110)).

The paper is organized as follows. Short potential model description adopted in this work is given in **Sec.2**. All results of this work with discussions are presented in **Sec.3**. The conclusions are summarized in **Sec.4**.

2. Calculation Method

Molecular dynamic is one of the most effective means to study the diffusion phenomena on different metallic surfaces [11,12]. In this work, we have calculated the adatom relaxation and also the bending energy at zero Kelvin by using molecular static calculations. The potential adopted in this study was based on the embedded atom method (EAM). Our systems are composed by Ag and Cu atoms. More precisely, our simulation box contains 8 layers, where each layer is formed by 64 atoms (8 atoms/row) as shown in Fig.1.

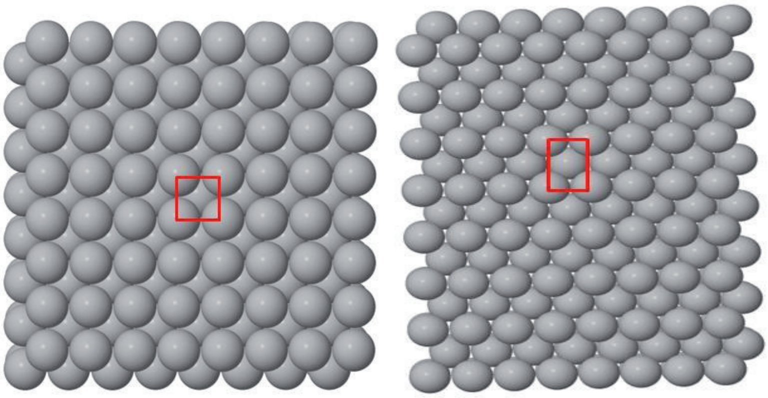

(a) (b)

Fig.1: Perspective view of the systems geometric structure studied in this work: (a) illustrates (100) surface geometry and (b) represents (110) surface geometry. The Square and the rectangular represent the adsorption sites (hollow).

In order to simulate an infinite system, periodic boundary conditions are applied in the direction parallel to the surface (x and y direction), but not in the perpendicular direction to the surface (z-direction). We mention also that the I calculations are made at 0K; therefore, temperature contributions are neglected. However, our investigations are carried out at static regime.

We note that in this study, we have adopted the embedded atom method (EAM) in order to solve our many-body problem [13]. This method has been used for many years ago in growth film area given good results [13]. In the framework of this method, the total energy of a metal is given as a sum of an embedding function $\mathrm{F_i(\rho_i)}$ and pair-potential $\mathrm{V_{ij}(R_{ij})}$ as:

$$\mathrm{E_{tot}} = \frac{1}{2}\sum_{\mathrm{i,j}} \mathrm{V_{ij}}\left(\mathrm{R_{ij}}\right) + \sum_{\mathrm{i}} \mathrm{F_i}(\rho_{\mathrm{i}}). \tag{1}$$

The quantity $\mathrm{R_{ij}}$ is the scalar distance between atom i and j, and ρ_{i} is the sum of individual electron density provided by the other atoms of the metal:

$$\rho_{\mathrm{i}} = \sum_{\mathrm{i(i \neq j)}} \rho_{\mathrm{j}}^{\alpha}(\mathrm{R_{ij}}). \tag{2}$$

In the following section we will examine the relaxation and length of the bond with and without adatom on (100) and (110) surfaces. We will try to find any possible correlation between bond length and the strength of bonding (binding energy).

3. Results

3.1. Substrate relaxation

The first step in this study is the examination of the top layer atom relaxation without adatom. For this investigation, we calculate the relaxation factor $\mathrm{d_p^*}$ as defined in Ref [14] by:

$$\mathrm{d_p^*} = \frac{\mathrm{d_{p,p+1}} - \mathrm{d^0_{p,p+1}}}{\mathrm{d^0_{p,p+1}}}, \tag{3}$$

Where$\mathrm{d_{p,p+1}}$ is the average distance between the first layer p and layer $\mathrm{p+1}$ after relaxation, and $\mathrm{d^0_{p,p+1}}$ is the corresponding unrelated distance.

We note that for Ag (100) and Cu (100) surfaces the relaxation factor $\mathrm{d_0^*}$ is found to be -2.2% and -3.9%, respectively. For Ag (100) surface the value of $\mathrm{d_0^*}$ is in good agreement with Boisvert et al. results [15], which is found to be -1.9% and in experiment results $d_0^* = 0 \pm 1.5$ [16]. For Cu (100) surface, d_p^* is reasonably compared with previous experiment and theoretical data (-3.6% [2], -4.5% [17],-3.5%[17],-3.0% [17],-3.02%[18],-1.2% [19]). One notes that, for surfaces without an adatom, all atoms in the same layer have the same vertical positions variation.

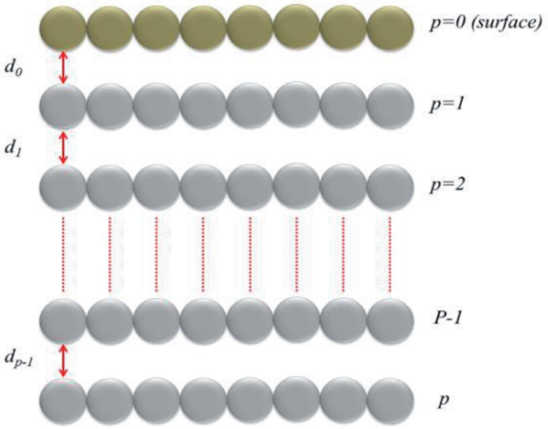

Fig. 2. Interlayer distance between substrate layers. The surface corresponds to the layer indexed by p=0.

For Ag(110), the relaxation of the top-layer is higher than that in Ag(100) surface and is found to be -5.25%. However, for Cu (110) surface, we have been found that d_0^* is -4.91%. We note that the top layer relaxation is very important in (110) substrate than (100). Consequently, the (100) surface is most compact than (110) surface.

3.2. Bond lengths and binding energies

a. On (100) surface

In this subsection we study the relaxation of the adatom on the (100) surface. For this specific investigation, we put an adatom on the surface and we follow the relaxation of its vertical position (Fig.1). For Cu/Cu (100), Ag/Ag (100) and Cu/Ag (100), the reduction of vertical position is -12.25%, -9.7% and -27.71%, respectively. We note that the adatom tries to be close of the surface and this is clearly showed in the reduction of vertical distance with the first nearest neighbors, this distance is the shortest for Cu on Ag (100) compared to the two others systems. While, for Ag on Cu (100), the adatom has an opposite behavior, and tends to be far from the surface. Thus, we observed that the vertical distance for this system with the nearest neighbor increases (+4.15%).

It is evident that the first nearest neighbors well feel the presence of the adatom more than the rest of the atoms in the layer. Thus, it is interesting to study their reaction after relaxation. On the (100) surface, for all systems, the first nearest neighbors of adatoms relax similarly and by occupying higher vertical positions than the rest of the atoms in the first layer (Fig. 3).

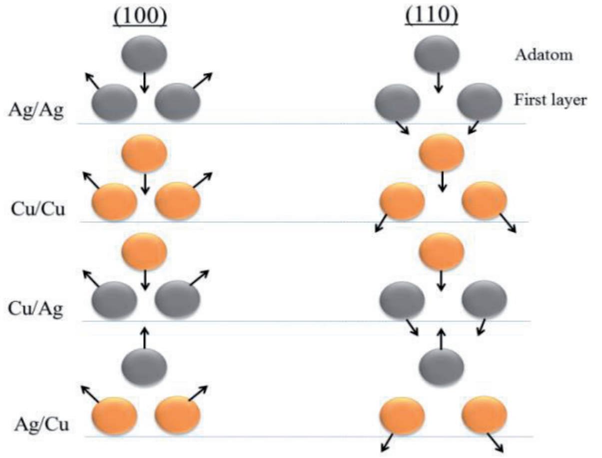

Fig.3. displacement orientation of adatom and the first nearest neighbors after relaxation

The bond length between the adatom and their first nearest neighbors is summarized in Table 1. For homoepitaxial systems, Ag on Ag (100), the bond length before relaxation is 2.89$\dot{A}$, so, after relaxation, it becomes shorter (2.81$\dot{A}$) by -4.49% which is in reasonable agreement with previous theoretical finding [2] (-5.4%). Similarly, for Cu on Cu (100), the bond length with first nearest after relaxation is 2.48$\dot{A}$ reduced by -5.47% from initial bond length (2.56$\dot{A}$) wish also still in good agreement with previous theoretical work [2] (-5.5%). For heteroepitaxial systems, the difference of the atomic size between adatoms and substrate atoms is clearly observed. For Cu on Ag (100), the adatom tries to reduce the bond length, and to be close to the substrate. In fact, the bond length before the relaxation is strongly reduced (-11.76%) with respect to the homoepitaxial systems. While for Ag on Cu(100), the bond length increases by a factor of 1.56%, indicating that the adatom attempts to be far from the substrate.

	100				
	Bond length (A°)				**E_{bind} (eV)**
Systems	**After relaxation**	**Before relaxation**	**Δd**	**%Δd**	**Adsorption position**
Ag/Ag	2.76	2.89	-0.13	-4.49	2
Cu/Cu	2.42	2.56	-0.14	-5.47	2.33
Cu/Ag	2.55	2.89	-0.34	-11.76	2.30
Ag/Cu	2.6	2.56	0.04	1.56	2.09

Table 1.Binding energies and Variation of bind length between adatom and the first neighbors on (100) surface.

In Table 1, we have also reported the binding energy values of adatom deposed on its favored adsorption position (around the first nearest neighbors).The binding energy per bond is found to be 0.50 eV for (Ag-Ag), and 0.58 eV for bond (Cu-Cu). In the case of heteroepitaxial systems, the binding energy is substantially higher for Cu on Ag (100) than for Ag on Cu (100). The binding energy per bond for Cu adatom on Ag (100) substrate is found to be 0.58 eV compared to (Cu-Cu) bond. If we change the Cu (100) substrate by Ag (100) surface, the binding energy for (Ag-Cu) bond is 0.50 eV. Also, the binding energy of Cu on Ag (100) is higher than that on Ag on Cu (100). Concerning (Ag-Cu) bond, the binding energy was influenced by the nature of the substrate; this is clearly seen in the binding energy when the substrate has been changed.

b. (110) surface

However, the reduction of vertical distance for Cu/Cu (110), Ag/Ag (110) and Cu/Ag (110) is found to be -18.85%, -13.45% and -35.58% respectively. We note also that the decrease of vertical distance between adatom and its first neighbors in (110) terrace is higher than in (100) surface, except for Ag on Cu, where we have the opposite behavior. On the other hand, our analysis of the relaxation of atoms on (110) surface, shows that the first nearest neighbors try to reduce their vertical position with the adatom, except for Ag on Cu (110) where the adatom and the first nearest neighbors have an opposite direction of relaxation (see Fig.1).

In addition, we have examined the bond length of the atoms in the systems for (110) surface (see again Table 2). The bond length between the Cu adatom and its first nearest neighbors on Cu (110) is found to be 2.48A. We also find that the bond length between Ag adatom and Ag (110) after relaxation is 2.81A. In the case of Cu adatom on Ag (110), the bond length decreases strongly than the other systems, this can be explained by the difference in the atomic size relative to adatom (copper and atoms of substrate silver). Therefore the decrease of (Cu-Ag) bond is about 8.65% relative to the bond length before relaxation (Table 2). This decrease is found to be close 2.77% for Ag on Ag (110) and 3.125% for Cu on Cu (110). While, for Ag adatom on Cu (110), as well as for Ag on Cu (100), the bond length increases with respect to the distance before relaxation by 2.73%, showing that the Ag adatom is repulsed far from the Cu surface.

	110				
	Bond length (A°)				**E_{bind} (eV)**
Systems	**After relaxation**	**Before relaxation**	**Δd**	**%Δd**	**Adsorption position**
Ag/Ag	2.81	2.89	-0.08	-2.77	2.11
Cu/Cu	2.48	2.56	-0.08	-3.125	2.53
Cu/Ag	2.64	2.89	-0.25	-8.65	2.42
Ag/Cu	2.83	2.56	0.07	2.73	2.3

Table 2.Binding energies and Variation of bind length between adatom and the first neighbors on (110) surface.

We have also reported in Table 2 the binding energy of adatom with the first nearest neighbors. As can be seen from the Table the binding energy per bond (Cu-Ag) is 0.62eV for Cu on Ag (110) and 0.575eV for Ag on Cu (110). For (Ag-Ag) and (Cu-Cu) bond, the binding energy per bond are 0.54 eV and 0.64 eV, respectively. Once again, we find that the binding energy is higher for Cu on Cu (110) and lower for Ag on Ag (110). From Table 2, we also remark that there is a correlation between the binding energy and bond length; we see that for Cu on Cu (110) the bond length is smaller than the other systems, whereas, it is smaller for Ag adatom both on Ag (110) and Cu (110) surface, where the bond length is higher.

4. Conclusions

This study contains important implications for the physics of thin film growth. We have found that the structure relaxation depends strongly on the surface orientation and on the nature of the substrate atoms. Thus, for (100) surface, the inter-layer relaxation is less important than in the case of the (110) orientation. Because, the (110) orientation offers wide free space than (100) surface. On the other hand, we have demonstrated that Cu adatom presents a strong reduction of the vertical position on both (100) and (110). These properties enhance significantly the exchange process occurring during Cu adatom diffusion. However, for both geometries considered here, the Ag adatom relaxation on Cu surface has an opposite behavior, where the adatoms are pushing far from the surface giving them a long lifetime on the surface. We mention that according to our finding in this work and our previous ones [1,4-6,12], we conclude that adatom diffusion depends on the nature of adatoms and also on the relaxation of adatom and the reaction of the first nearest neighbors. This observation has been confirmed by the calculation of the bending energy, where we have found that Cu adatom needs more energy to be snatched from its initial position on Ag surface. On the other side, it's very hard to emerge Ag adatom on Cu surface.

Acknowledgment

We gratefully acknowledge the financial support from CNRST-Maroc to the university of Chouaïb Doukkali (contract: 104/2009) under the program "Material sciences". We also thank Professor Abdelkader KARA (from University of Central Florida) for scientific discussions.

References

[1] K. Sbiaai, Y. Boughaleb, M. Mazrouiand A. Kara. Surface and Interface Analysis, 2013, 45, 1702–1708.

[2] H. Yildirim and T. S. Rahman, Phys. Rev. B. 2009, 80, 235413.

[3] S. Cereda and F. Montalenti, Phys. Rev. B, 2010, 81, 125439.

[4] K. Sbiaai, Y. Boughaleb, J -Y. Raty, A. Hajjaji, M. Mazroui, A. Kara, J. Optoelectron. Adv. M. 2012, 14, 1059 – 1065.

[5] K. Sbiaai, J. Optoelectron. Adv. M. 2013, 15, 501 – 504.

[6] C.T. Langlois, T. Oikawa, P. Bayle-Guillemaud, C. Ricolleau, J. Nanopart. Res. 2008, 10, 997 – 1007.

[7] T.R. Linderoth, S. Horch, E. Laegsgaard, I. Stensgaard, F. Besenbacher, Surf. Sci. 1998, 402–404, 308.

[8] H. Yildirim, A. Kara, T.S. Rahman, Phys. Chem. C, 2012, 116, 281–291.

[9] D. Bochicchio, R. Ferrando, Nano Lett. 2010, 10 4211–4216.

[10] T.R. Linderoth, S. Horch, E. Laegsgaard, I. Stensgaard, F. Besenbacher, Phys. Rev. Lett. 1997, 78, 4978.

[11] F. Montalenti, R. Ferrando, Surf. Sci. 1999, 433 455.

[12] K. Sbiaai, Y. Boughaleb, M. Mazroui, A. Hajjaji, A. Kara, Thin Solid Films, 2013, 548, 331-335.

[13] M. Daw, M.I. Baskes, Phys. Rev. B, 1984, 29, 6443.

[14] C. Mottet and G. Tréglia and B. Legrand. Phys. Rev. B, 1992, 46, 16018.

[15] G. Boisvert and L. J. Lewis, Phys. Rev. B, 1995, 52, 9078.

[16] H. Li, J. Quinn, Y.S. Li, D. Tian, F. Jona, and P.M. Marcus, Phys. Rev. B, 1991, 43, 7305.

[17] G. Boisvert and L. J. Lewis, Phys. Rev. B, 1997, 56, 7643.

[18] Th. Rodach, K.-P.Bohnen, and K. M. Ho, Surf. Sci. 1993, 286, 66.

[19] D. M. Lind, F. B. Dunning, G. K. Walters, and H. L. Davis, Phys. Rev. B, 1987, 35, 9037.

Instructions for authors

1. Type of Manuscripts
2. Organization of the Manuscript
3. Language
4. Submission of the Manuscript
5. Peer Review
6. Revision of the Manuscript
7. Special Features, Appendices and Supplementary Material
8. Preprint Option
9. Publication of the Manuscript

Frontiers in Science and Engineering an International Journal edited by Hassan II Academy of Science and Technology uses author-supplied PDFs for all online and print publication.

1. Type of Manuscripts

The FSE Journal publishes the following article types :

Reviews/State of the art, usually through Academy invitation and organized into themed issues, report on recent advances in science and technology. 20 pages maximum according to the format given.

Original Research Papers contain innovative and hypothesis-driven research; supported by sound experimental design, methodology, proofs, and data interpretation. 16 pages maximum according to the format given.

Letters to the Editor: May be submitted by readers commenting articles already published by the Journal. 1 to 2 pages maximum according to the format given.

2. Organization of the Manuscript

The entire manuscript, including mathematical equations, flow-sheets, chemical structures, tables, and figures must be prepared in electronic form and submitted as pdf files. Use Times New Roman size 12. For all special characters (e.g., Greek characters) use the font Symbol. Use carriage returns only to end headings and paragraphs, not to break lines of text. Automatic hyphenation should be turned off. Do not insert spaces before punctuation. Verify the correct spelling for the final version with the Spelling and Grammar function of Word.

3. Language

Manuscripts should be written in English.

4. Submission of the Manuscript

The manuscript and supplementary material must be send by the corresponding author to the Editor in an electronic form as pdf files.

You may be required to register as a new user within the Publication System Manager upon your first visit. Straightforward login and registration procedures can be found on the website. Editorial Manager allows authors to track the progress of manuscript review in real time. Detailed, step-by-step instructions for submitting manuscripts can be found on the website. All correspondence regarding your manuscript must go through Publication System Manager.

Authors are asked to prepare their papers, and PDF files, according to the templates and guidelines provided below.

The author(s) need to supply the following items :

- the PDF file of the paper
- a signed Assignment of Copyright Form (once the paper accepted)

We highly recommend that authors prepare their papers/PDFs using the following Microsoft Word or LaTeX templates, which can be downloaded from the following links :

- Microsoft guidelines and templates
- Latex guidelines and class file

A copyright license form will be provided to the corresponding author only when a paper is accepted for publication.

5. Peer Review

All submissions will be reviewed anonymously by at least two independent referees, and a referee should never communicate directly with an author. A referee must treat as confidential material the manuscript and any supplementary material. Authors may suggest names and email addresses of expert reviewers, but selection remains a prerogative of the Editors. Authors may include supplementary notes to facilitate the review process. If an accepted paper is cited that has not yet appeared in print and is required for evaluation of the submitted manuscript, authors should provide an electronic version for use by the Reviewers. Authors are responsible for all statements in their work, including changes made by the copy editor after a manuscript is accepted.

6. Revision of the Manuscript

All comments made by referees must be addressed. A letter describing all changes that were made should be attached with the revised version of the manuscript. A copyright license form must accompany the final version of the manuscript.

7. Special Features, Appendices and Supplementary Material

Special features containing highly interactive features or large databases can be included. All authors are encouraged to take advantage WEB online publishing capabilities (i.e. 3-D, video, and interactive graphics). All special features must be created by the Author›s).

Authors who wish to publish electronic supplementary material to their article (Excel files, images, audio/video files) must submit the supplementary files/materials with their manuscript submission via our online peer review tracking Publication System Manager. Note that supplementary files are not automatically included in the reviewer PDF. Please therefore note in the cover letter if these materials should be evaluated by reviewers.

8. Preprint Option

Before making a PDF file of your article, please check the following tips in the next section.

Article checklist

There are a number of essential basic requirements which must be followed during preparation of your article. If article PDFs are prepared without following these essential requirements, publication may be delayed until a usable and compatible PDF is received.

Articles must not contain page numbers, headers or footers

This is extremely important. Page numbers, copyright details etc are added by the Publication System Manager Publishing during the production and publication process. If you put page numbers on your paper we will have to contact you for a replacement PDF, which could delay publication.

Article margins must be adequate

We recommend a minimum 15mm all round. The Microsoft Word template or Latex templates automatically provide the correct margins so their use is highly recommended.

All articles must have an abstract

When readers are searching for information online, an abstract of an article is the first thing they see. Your abstract needs to be concise but convey as much information as possible about the content of your article. In addition, our Publication System Manager Publishing will supply your abstract to many other database systems used by researchers to find papers.

Addresses should be complete and include the country and a contact name

The title of the article, author names with full first name (no degrees), each author’s affiliation, and a suggested running head (of less than 50 characters, including spaces). The affiliation should comprise the department, institution (usually university or company), city, and country and should be typed as a footnote to the author’s name. For the corresponding author designated to correspond with the Editorial Office and review proofs, indicate his/her complete mailing address, office/cellular telephone number, fax number, and e-mail address. During production of the electronic paper we may need to contact you if there is something to check or for a request a replacement PDF file.

References should be complete and carefully formatted

Online versions of all reference lists will, wherever possible, be electronically linked to the articles that you cite. Reference lists containing many links direct to the cited paper are a valuable research tool. The time and effort spent in preparing your references, so that they can be linked, will be very appreciated by readers of your paper. Please, notice also that all the citations should be justified according to the contents of the proposed article. Abusive citations of the same author may induce a certain delay in the overall review process

PrePrint

Any manuscript received for publication in FSE can be published on the Web as preprint. All authors submitting a manuscript must clearly indicate that they wish to publish it as a preprint. The referees appreciate if the manuscript meets the basic requirements for publication and recommend its publication as preprint. A preprint not accepted for publication by the referees will be immediately removed from the preprint collection. A published paper which was previously available as a preprint will have clearly indicated the date when it was first published on the Web. A work published as preprint can benefit from comments from the readers which can eventually improve the manuscript. Revised versions that incorporate corrections from reviewers and suggestions from readers can be also published as preprints.

9. Publication of the Manuscript

Accepted papers are published as PDF files available at the Web site of the Academy.

Transfer of Copyright Form

A signed copy of the Transfer of Copyright must be submitted online as part of the manuscript submission process (FSECopyright.pdf).

Astract

Reviews/State of the Art, Original Research Articles, require an abstract. The abstract is limited to 300 words or less. For Research Articles, the abstract should include a brief statement for each of the sections related to Introduction, Methods/Approaches/Materials and Discussion, and Conclusion written in paragraph form. All abstracts must be written in one paragraph, with no subheadings, equations, tables, reference citations or graphics.

Keywords

Provide a list of no more than 5 key words.

Introduction

Required for Reviews/State of the art and Original Research Articles.

Main Text Body

For Original Research Articles, organize the main text as follows: Introduction, Approach/Materials and Methods, Results, Discussion, and Conclusion. The use of subheadings to divide the text is encouraged. Primary, Secondary, and Third level headings should be clearly defined, but do not use numbers or letters.

Recommended word counts are as follows: Reviews/State of the art: 8000, Original Research Articles : 6000.

Use abbreviations sparingly, and define them at the first insertion in the text. Use the metric system for all measurements. Express metric abbreviations in lowercase letters without periods (cm, ml, sec). Define all symbols used in equations and formulas. When symbols are used extensively, the authors may include a list of all symbols in a table.

Conclusion

The conclusion should be a brief paragraph, containing 3 to 4 sentences, that summarizes the findings presented.

Acknowledgments

Include funding source(s) and other contributions. If the work has been funded by any organisation please provide name(s) of funding institute(s) and grant number(s).

References

References should conform to Vancouver style and be numbered consecutively in the order in which they are cited in the text. Cite in the text by the appropriate Arabic numeral enclosed in parentheses, e.g., (1), (2-5), etc.

It is advisable to limit the maximum number of references as really needed only.

References to unpublished peer-reviewed, personal communications, including conference abstracts, and papers in preparation or in review, cannot be listed, but can be notated parenthetically in the text.

Abbreviations for journal names should conform to those of Vancouver style (as depicted in http://www.library.uq.edu.au/training/citation/vancouv.pdf). The style and punctuation of the references should conform to conventional referencing.

Whenever, the paper is not yet published officially but accepted, please write down the corresponding DOI within the reference.

Authors may identify uniform resource locators (URLs) for websites that provide the reader with additional information on the topic addressed in the manuscript. Although URLs are an important feature of electronic publishing, authors are encouraged to be very selective in their choice of sites to include. Do not include links to sites that are not accessible without a password.

All on-line documents should contain author(s), title, On-line document/ Web /FTP /organisation /On-line database/ Supplementary material/ Private homepage , and Accessed Day Month Year, so that readers can refer to.

Tables

Tables must be created in Microsoft Word /Latex table format. Tables should be numbered (with Roman numerals) and referred to by number in the text. Center the title above the table, and type explanatory footnotes (indicated by superscript lowercase letters) below the table. Data must be placed in separate cells of the table to prevent text and numbers from shifting when the table is converted for publication on the Internet. Empty cells may be inserted to create spacing. Tables should not duplicate information provided in the text. Instead, tables should be used to provide additional information that illustrates or expands on a specific point the author wishes to make. Each table should be self-explanatory.

Figures

The FSE offers authors the use of color figures in online published manuscripts. Figures (as well as photographs, drawings, diagrams, and charts) are to be numbered in one consecutive series of Arabic numerals in the order in which they are cited in the text. All Electronic artwork must be submitted online via our online peer review tracking system, Publication System Manager.

The maximum combined count for tables and figures for papers should not exceed 15 to 20.

Footnotes

Footnotes should be avoided. When their use is absolutely necessary, footnotes should be numbered consecutively using Arabic numerals and should be typed at the bottom of the page to which they refer. Place a line above the footnote, so that it is set off from the text. Use the appropriate superscript numeral for citation in the text.

Guidelines

We highly recommend that authors prepare their papers/PDFs using the following Microsoft Word or LaTeX templates, which can be downloaded from the following links:

- Latex guidelines and class file http://www.academie.hassan2.sciences.ma/fse/FSE%20Sample%20cls.tex.txt

- PDF guidelines and templates http://www.academie.hassan2.sciences.ma/fse/FSE%20Sample%20cls.pdf

- Microsoft word guidelines and templates

Contractual issues

1. Full Disclosure

During the manuscript submission process, all authors will be required to confirm that the manuscript has not been previously published in any language anywhere and that it is not under simultaneous consideration by another journal.

2. Conflicts of Interest

Authors must declare all conflicts of interest (or their absence) in their cover letter upon submission of a manuscript. This conflict declaration includes conflicts or potential conflicts of all listed authors. If any conflicts are declared, FSE publish them with the paper. In cases of doubt, the circumstance should be disclosed so that the editors may assess its significance.

Conflicts may be financial, academic, commercial, political or personal. Financial interests may include employment, research funding (received or pending), stock or share ownership, patents, payment for lectures or travel, consultancies, nonfinancial support, or any fiduciary interest in a company.

3. Copyright Transfer

The Copyright Revision Act requires that Authors transfer their copyrights to the Publisher, HIIAST, in order to provide for the widest possible dissemination of professional and scientific literature. A signed Transfer of Copyright form must be submitted online with the manuscript. The Transfer of Copyright form for an accepted manuscript must be on file with the HIIAST Editorial Office prior to production for publication. Corresponding Authors may print and sign the form on behalf of all authors The Transfer of Copyright form can be found at fsecopyright.pdf.

4. Use of Copyrighted Tables and Figures

A copy of the granted permission to use copyrighted figures and tables must be included with the submitted manuscript.

Dépôt légal : 2012 PE 0007
ISSN : 2028 - 7615

ACADEMY Press MA

Email : fse@academiesciences.ma
www.academiesciences.ma/fse/